REPORT DOCUMENTATION PAGE

Form Approved
OMB No. 0704-0188

1. REPORT DATE *(DD-MM-YYYY)*	**2. REPORT TYPE**	**3. DATES COVERED** *(From - To)*
15 May 2005	Journal Article POSTPRINT	2004

4. TITLE AND SUBTITLE
Coupled energy-drift and force-balance equations for high-field hot-carrier transport

5a. CONTRACT NUMBER

5b. GRANT NUMBER

5c. PROGRAM ELEMENT NUMBER

6. AUTHOR(S)
Danhong Huang, P.M. Alsing, T. Apostolova, D.A. Cardimona

5d. PROJECT NUMBER
2304

5e. TASK NUMBER
CR

5f. WORK UNIT NUMBER
A1

7. PERFORMING ORGANIZATION NAME(S) AND ADDRESS(ES) AND ADDRESS(ES)
Air Force Research Laboratory
Space Vehicles
3550 Aberdeen Ave SE
Kirtland AFB, NM 87117-5776

8. PERFORMING ORGANIZATION REPORT NUMBER
AFRL-VS-PS-JA-2006-1006

9. SPONSORING / MONITORING AGENCY NAME(S) AND ADDRESS(ES)

10. SPONSOR/MONITOR'S ACRONYM(S)

11. SPONSOR/MONITOR'S REPORT NUMBER(S)

12. DISTRIBUTION / AVAILABILITY STATEMENT
Approved for public release; distribution is unlimited. (VS05-0024)

13. SUPPLEMENTARY NOTES
Published in Physical Review B (Condensed Matter and Materials Physics); 15 May 05; vol.71, no.19, p.195205-1 – 13.

14. ABSTRACT
Coupled energy-drift and force-balance equations that contain a frictional force for the center-of-mass motion of electrons are derived for hot-electron transport under a strong dc electric field. The frictional force is found to be related to the net rate of phonon emission, which takes away the momentum of a phonon from an electron during each phonon-emission event. The net rate of phonon emission is determined by the Boltzmann scattering equation, which depends on the distribution of electrons interacting with phonons. The work done by the frictional force is included into the energy-drift equation for the electron-relative scattering motion and is found to increase the thermal energy of the electrons. The importance of the hot-electron effect in the energy-drift term under a strong dc field is demonstrated in reducing the field-dependent drift velocity and mobility. The Doppler shift in the energy conservation of scattering electrons interacting with impurities and phonons is found to lead to an anisotropic distribution of electrons in the momentum space along the field direction. The importance of this anisotropic distribution is demonstrated through a comparison with the isotropic energy-balance equation, from which we find that defining a state-independent electron temperature becomes impossible. To the leading order, the energy-drift equation is linearized with a distribution function by expanding it into a Fokker-Planck-type equation, along with the expansions of both the force-balance equation and the Boltzmann scattering equation for hot phonons.

15. SUBJECT TERMS
Boltzmann equation; Carrier mobility; Doppler shift; Electron phonon interactions; Fokker Planck equation; Hot carriers; Frictional force; Electron motion; Hot electron transport; Phonon emission; Electrons distributions; Energy drift equation; Momentum space

16. SECURITY CLASSIFICATION OF:			**17. LIMITATION OF ABSTRACT**	**18. NUMBER OF PAGES**	**19a. NAME OF RESPONSIBLE PERSON**
a. REPORT	**b. ABSTRACT**	**c. THIS PAGE**			David A. Cardimona
Unclassified	Unclassified	Unclassified	Unlimited	14	**19b. TELEPHONE NUMBER** *(include area code)* 505-846-5807

Coupled energy-drift and force-balance equations for high-field hot-carrier transport

Danhong Huang, P. M. Alsing, T. Apostolova, and D. A. Cardimona
Air Force Research Lab, Space Vehicles Directorate, Kirtland Air Force Base, New Mexico 87117, USA
(Received 9 December 2004; published 25 May 2005)

Coupled energy-drift and force-balance equations that contain a frictional force for the center-of-mass motion of electrons are derived for hot-electron transport under a strong dc electric field. The frictional force is found to be related to the net rate of phonon emission, which takes away the momentum of a phonon from an electron during each phonon-emission event. The net rate of phonon emission is determined by the Boltzmann scattering equation, which depends on the distribution of electrons interacting with phonons. The work done by the frictional force is included into the energy-drift equation for the electron-relative scattering motion and is found to increase the thermal energy of the electrons. The importance of the hot-electron effect in the energy-drift term under a strong dc field is demonstrated in reducing the field-dependent drift velocity and mobility. The Doppler shift in the energy conservation of scattering electrons interacting with impurities and phonons is found to lead to an anisotropic distribution of electrons in the momentum space along the field direction. The importance of this anisotropic distribution is demonstrated through a comparison with the isotropic energy-balance equation, from which we find that defining a state-independent electron temperature becomes impossible. To the leading order, the energy-drift equation is linearized with a distribution function by expanding it into a Fokker-Planck-type equation, along with the expansions of both the force-balance equation and the Boltzmann scattering equation for hot phonons.

DOI: 10.1103/PhysRevB.71.195205 PACS number(s): 61.80.Az, 72.20.Ht, 61.82.Fk, 72.10.Di

I. INTRODUCTION

There have been many theories proposed over the years to describe the transport of hot electrons through a solid when the electric field being applied to the system is large, and the current-voltage characteristics deviate from those of linear response theory. The semiclassical (regular) Boltzmann transport equation, with momentum-drift included, seems to be the only one of these early theories amenable to practical use. However, even the regular Boltzmann transport equation becomes laborious when the system goes beyond the linear-field regime. Frölich and Paranjape[1] used a displaced Maxwellian distribution to describe the electron transport in insulators and semiconductors at high temperatures. Later, Arai[2] used a similar model to describe electron transport in metals at low temperatures, using a Fermi-Dirac distribution instead to predict a finite electron temperature under an applied electric field, even when the lattice temperature went to zero. Soon after that, Lei and Ting[3] proposed coupled force-balance and energy-balance equations to describe electrons in semiconductors and metals at both low and high temperatures by assuming an isotropic quasi-thermal-equilibrium (Fermi-Dirac) distribution for hot electrons with a temperature different from the lattice temperature. Very recently, Huang *et al.*[4] used the Boltzmann scattering equation to replace the energy-balance equation, and then accurately determined the electron temperature.

It is well known that the drifting of electrons under a dc field can be treated as a field-driven center-of-mass (collective) motion of many electrons.[5] The scattering of electrons by the lattice ions or impurities within the lattice can then be considered as a relative motion within the center-of-mass frame. A spatially-uniform external field will only couple to the center-of-mass motion. The lattice ions and the ionized impurity atoms within the semiconductor remain stationary with respect to the moving center of mass. The center-of-mass motion will couple to the relative scattering motion through a Doppler shift in the electron energy along the field direction. This can be modeled as a frictional force acting between the drifting electrons and the stationary lattice and impurity atoms.[3] As a result, the motion of the electrons under a dc field will be effectively opposed by this friction. Even though this frictional force can be measured classically, it is a quantum-statistical average of all the frictional forces acting on all the electrons in the relative scattering motion, and thus it depends on the distribution of electrons in different quantum states. This distribution of electrons in the various quantum states is determined by the Doppler-shift-modified elastic and inelastic scattering of the electrons, including phonon and impurity scattering.

The most straightforward and simplest way to treat a steady-state distribution of electrons is by introducing a state-independent electron temperature for use in a Fermi-Dirac distribution of hot electrons. This electron temperature, different from the lattice temperature, can be found by using an isotropic energy-balance equation for the relative motion of the electrons.[3] However, this simple method cannot be used when an external field is present, even in a steady state, since in that case, the assumption of an isotropic Fermi-Dirac distribution for hot electrons cannot be justified. Indeed, the energy-balance equation itself cannot be justified when the drift velocity is large, producing a Doppler shift that is comparable to the phonon energy. Finally, even though the energy-balance equation can include the screening effect, it excludes the effects of electron-electron scattering on electron transport. For these reasons, we introduce a more rigorous method to describe the relative motion of hot electrons undergoing anisotropic scattering that involves the use of the Boltzmann scattering equation, with the addition of an energy-drift term. When the dc electric field is very strong,

the distribution of hot electrons is far from equilibrium, and the definition of a state-independent electron temperature becomes impossible. Therefore, the approximate treatments[3,6] of hot phonons are no longer valid.

The motivation of the current paper is as follows. It is known that the regular Boltzmann transport equation includes carrier drift in momentum space, but does not apply to hot-carrier transport under a strong dc field. On the other hand, the energy-balance equation includes hot-carrier effects, but the isotropic carrier distribution that is assumed does not include any anisotropic momentum dependence in the carrier distribution along the field direction; the state-independent electron temperature that is introduced becomes unphysical when the dc field is very strong, and the conditions are far from equilibrium. We propose coupled energy-drift and force-balance equations that can be applied to hot-carrier transport by including both the hot-carrier effects and the anisotropic momentum dependence in the carrier distribution along the field direction, without introducing a state-independent electron temperature.

The energy-drift and force-balance equations proposed here are based on the following physical considerations:

(i) Transport of carriers under a dc field results from the center-of-mass drifting motion. This slow motion can be treated classically after a quantum-statistical average has been taken.

(ii) Interaction between moving carriers and static lattice ions and static impurity atoms in a motion relative to the center of mass is modified by a Doppler shift in the energy of the moving carriers in the field direction. This couples the center-of-mass motion with the relative motion.

(iii) The relative scattering motion of the carriers becomes anisotropic in the field direction due to the Doppler shift. This contributes to a nonzero frictional force that resists the dc-driving force. This frictional force contains contributions from impurities and phonons. The phonon-emission process will take the momentum of a phonon away from a carrier, while the phonon-absorption process will add the momentum of a phonon to a carrier.

(iv) The classical center-of-mass motion can be described by the force-balance equation including a frictional force, while the relative motion is composed of many-particle quantum-scattering events that can be described by the energy-drift equation, including the work done by the frictional forces to increase the thermal energy of the carriers. The increased thermal energy of hot carriers is expected to reduce the field-dependent carrier drift velocity and mobility.

In this paper, we have generalized our theory in Ref. 4 by using the Boltzmann scattering equation with energy drift included and by using momentum dissipation in the representation of the phonon-induced frictional scattering forces. This allows us to completely eliminate the need for any sort of electron- and lattice-temperature definitions, and allows us to describe events far from equilibrium. This approach also brings the hot-electron transport formulation closer to that of the semiconductor Bloch equations,[7] which should allow the coupling of these two formalisms to proceed without any problems when coherent optical interactions are included in the future.

The organization of the paper is as follows. In Sec. II, we introduce our model and theory, and derive coupled energy-drift and force-balance equations for hot-carrier transport under a strong dc electric field. The numerical results are displayed in Sec. III for the calculated drift velocities and mobilities as functions of the dc field, and they are explained physically. The paper is concluded in Sec. IV along with some remarks.

II. THEORY

The motion of many electrons in *n*-doped bulk semiconductors can be separated into the center-of-mass and relative scattering motions. The center-of-mass motion of electrons is described by a Newton-like force-balance equation for the drift velocity of the center of mass. The forces in this equation contain a driving force from a dc electric field and a frictional force from both impurity and phonon scattering. During the scattering of electrons with phonons, each phonon-emission process takes away the momentum of a phonon from an electron. Meanwhile, each phonon-absorption process adds the momentum of a phonon to an electron. The relative scattering motion of electrons should be described by the energy-drift equation, i.e., the Boltzmann scattering equation without momentum drift included, but with energy drift included. The energy drift is due to the work done by the frictional force against the center-of-mass drift motion of the electrons. This work increases the internal energy (i.e., the thermal energy) of electrons, causes the distribution of electrons to deviate from an equilibrium one, and reduces the mobility of hot electrons due to enhanced scattering with phonons. When the dc field is weak, the phonons are described by a distribution that is nearly in equilibrium. However, when the dc field is strong, the phonons are described by a nonequilibrium distribution. For this latter case, many phonons must be generated to balance the strong dc-driving force.

In order to make this paper self-contained, we will rewrite some of the key equations from Ref. 4 in a slightly more general form. In the presence of a spatially-uniform dc electric field $\vec{E}_{\rm dc}$, the Hamiltonian of many *interacting* electrons in bulk semiconductors can be written as

$$\mathcal{H}=\frac{1}{2m^*}\sum_i \hat{\vec{p}}_i^{\,2}+\sum_{i<j}\frac{e^2}{4\pi\epsilon_0\epsilon_{\rm r}|\vec{r}_i-\vec{r}_j|}-e\sum_i \vec{r}_i\cdot\vec{E}_{\rm dc}+\sum_{i,a}U^{\rm imp}(\vec{r}_i-\vec{R}_a)-\sum_{i,\ell}\vec{u}_\ell\cdot\vec{\nabla}_{\vec{r}_i}U^{\rm ion}(\vec{r}_i-\vec{R}_\ell), \quad (1)$$

where $i=1,2,\ldots,N_e$ is the index of N_e electrons, $a=1,2,\ldots,N_a$, is the index for N_a impurity atoms, $\ell=1,2,\ldots,N_\ell$ is the index for N_ℓ lattice ions, $\vec{r}_i$ is the position vector for the ith electron, $\vec{R}_a$ and $\vec{R}_\ell$ are the position vectors of impurity atoms and lattice ions, $\vec{u}_\ell$ represents the ion displacement from the thermal equilibrium position, m^* is the effective mass of electrons, ϵ_0 is the dielectric constant in the vacuum, and ϵ_r is the relative dielectric constant of host semiconductors. The single-electron momentum operator is $\hat{\vec{p}}_i=-i\hbar\vec{\nabla}_{\vec{r}_i}$, and both the impurity potential $U^{\rm imp}(\vec{r}_i-\vec{R}_a)$ and the ion potential $U^{\rm ion}(\vec{r}_i-\vec{R}_\ell)$ are included. We first define the center-of-mass momentum and position vectors by

$$\hat{\vec{P}}^{\rm c}=\sum_i \hat{\vec{p}}_i, \quad \vec{R}^{\rm c}=\frac{1}{N_e}\sum_i \vec{r}_i, \tag{2}$$

and those for the relative motion by

$$\hat{\vec{p}}_i'=\hat{\vec{p}}_i-\frac{1}{N_e}\hat{\vec{P}}^{\rm c}, \quad \vec{r}_i'=\vec{r}_i-\vec{R}^{\rm c}. \tag{3}$$

By using the center-of-mass and relative momentum and position vectors defined in Eqs. (2) and (3), we can separate the total Hamiltonian, including the Hamiltonians of electrons and phonons, into one center-of-mass Hamiltonian $\mathcal{H}_{\rm cm}$ and another relative Hamiltonian $\hat{\mathcal{H}}_{\rm rel}$, given by

$$\mathcal{H}_{\rm cm}=\frac{(\hat{\vec{P}}^{\rm c})^2}{2N_e m^*}-N_e e\vec{E}_{\rm dc}\cdot\vec{R}^{\rm c}, \tag{4}$$

$$\begin{aligned}\hat{\mathcal{H}}_{\rm rel}=&\sum_{\vec{k},\sigma}\varepsilon_k\hat{a}^\dagger_{\vec{k}\sigma}\hat{a}_{\vec{k}\sigma}+\sum_{\vec{q},\lambda}\hbar\Omega_{q\lambda}\hat{b}^\dagger_{\vec{q}\lambda}\hat{b}_{\vec{q}\lambda}\\&+\frac{1}{2}\sum_{\vec{k},\vec{k}',\sigma,\sigma'}\sum_{\vec{q}}\frac{e^2}{\epsilon_0\epsilon_r q^2\mathcal{V}}\hat{a}^\dagger_{\vec{k}+\vec{q}\sigma}\hat{a}^\dagger_{\vec{k}'-\vec{q}\sigma'}\hat{a}_{\vec{k}'\sigma'}\hat{a}_{\vec{k}\sigma}\\&+\sum_{\vec{k},\sigma}\sum_{\vec{q},\lambda}C_{q\lambda}(\hat{b}_{\vec{q}\lambda}+\hat{b}^\dagger_{-\vec{q}\lambda})e^{i\vec{q}\cdot\vec{R}^{\rm c}}\hat{a}^\dagger_{\vec{k}+\vec{q}\sigma}\hat{a}_{\vec{k}\sigma}\\&+\sum_{\vec{k},\sigma}\sum_{\vec{q},a}U_{\rm i}(q)e^{i\vec{q}\cdot(\vec{R}^{\rm c}-\vec{R}_a)}\hat{a}^\dagger_{\vec{k}+\vec{q}\sigma}\hat{a}_{\vec{k}\sigma},\end{aligned} \tag{5}$$

where $\mathcal{V}$ is the volume of the system, $\hbar\Omega_{q\lambda}$ is the phonon energy with wave number q for mode λ (totally three modes), $\varepsilon_k=\hbar^2k^2/2m^*$ is the kinetic energy of electrons with wave number k, and the index $\sigma=\pm1$ is for the up-and down-spin states of electrons. We use $\hat{a}^\dagger_{\vec{k}\sigma}$ ($\hat{a}_{\vec{k}\sigma}$) to represent the creation (annihilation) operator of electrons and $\hat{b}^\dagger_{\vec{q}\lambda}$ ($\hat{b}_{\vec{q}\lambda}$) to denote the creation (annihilation) operator of phonons. $U_{\rm i}(q)$ is the Fourier transform of the impurity potential $U^{\rm imp}(\vec{r}'+\vec{R}^{\rm c}-\vec{R}_a)$, and $C_{q\lambda}$ is the electron-phonon coupling constant that will be given later in this section. The coupling of the center-of-mass and relative motions [the factor $\exp(i\vec{q}\cdot\vec{R}^{\rm c})$] can be seen from the impurity and phonon parts of the relative Hamiltonian in Eq. (5).

From the total Hamiltonian, we derive two Heisenberg equations for the center-of-mass motion of electrons,

$$\begin{aligned}\frac{d}{dt}\hat{\vec{P}}^{\rm c}=&\frac{1}{i\hbar}[\hat{\vec{P}}^{\rm c},\mathcal{H}_{\rm cm}+\hat{\mathcal{H}}_{\rm rel}]=N_e e\vec{E}_{\rm dc}-i\sum_{\vec{q},\lambda}C_{q\lambda}\vec{q}e^{i\vec{q}\cdot\vec{R}^{\rm c}}\\&\times(\hat{b}_{\vec{q}\lambda}+\hat{b}^\dagger_{-\vec{q}\lambda})\hat{\rho}_{\vec{q}}-i\sum_{\vec{q},a}U_{\rm i}(q)\vec{q}e^{i\vec{q}\cdot(\vec{R}^{\rm c}-\vec{R}_a)}\hat{\rho}_{\vec{q}},\end{aligned} \tag{6}$$

$$\hat{\vec{u}}=\frac{d}{dt}\vec{R}^{\rm c}=\frac{1}{i\hbar}[\vec{R}^{\rm c},\mathcal{H}_{\rm cm}+\hat{\mathcal{H}}_{\rm rel}]=\frac{\hat{\vec{P}}^{\rm c}}{N_e m^*}, \tag{7}$$

where $\hat{\rho}_{\vec{q}}=\Sigma_{\vec{k},\sigma}\hat{a}^\dagger_{\vec{k}+\vec{q}\sigma}\hat{a}_{\vec{k}\sigma}$ represents the density-wave operator of electrons. Applying a quantum-statistical average $\langle\langle\cdots\rangle\rangle_{\rm av}$ to Eqs. (6) and (7) and defining the following quantities:

$$N_e m^*\frac{d}{dt}\vec{u}_0\equiv\left\langle\left\langle\frac{d}{dt}\hat{\vec{P}}^{\rm c}\right\rangle\right\rangle_{\rm av}, \tag{8}$$

where $\vec{u}_0\equiv\langle\langle\hat{\vec{P}}^{\rm c}/N_e m^*\rangle\rangle_{\rm av}$ is the drift velocity related to the center-of-mass momentum, we obtain the following force-balance equation:

$$N_e m^*\frac{d}{dt}\vec{u}_0=N_e e\vec{E}_{\rm dc}+\vec{F}_{\rm i}[\vec{u}_0]+\vec{F}_{\rm p}[\vec{u}_0]. \tag{9}$$

Here $\vec{F}_{\rm i}[\vec{u}_0]$ and $\vec{F}_{\rm p}[\vec{u}_0]$ are the frictional forces resulting from impurity and phonon scattering, respectively.

For the relative motion of electrons, the energy-drift equation for electrons in a dc field can be derived as[8]

$$\begin{aligned}\frac{dn_{\vec{k}}}{dt}=&\pi\sum_{\vec{q}}(\vec{q}\cdot\vec{u}_0)N_a|U_{\rm i}(q)|^2\delta(\varepsilon_{k+q}-\varepsilon_k+\hbar\vec{q}\cdot\vec{u}_0)\frac{\partial}{\partial\varepsilon_k}(n_{\vec{k}+\vec{q}}-n_{\vec{k}})+\frac{\hbar}{2}\sum_{\vec{q},\lambda}(\vec{q}\cdot\vec{u}_0)\left\{[N_{\vec{q}\lambda}(\omega_{q\lambda})+1]\left\{\frac{\partial}{\partial\varepsilon_k}\right\}_{[n]}\Theta^{\rm em}_{\vec{k},\vec{q}\lambda}-N_{\vec{q}\lambda}(\omega_{q\lambda})\right.\\&\left.\times\left\{\frac{\partial}{\partial\varepsilon_k}\right\}_{[n]}\Theta^{\rm abs}_{\vec{k},\vec{q}\lambda}\right\}+\frac{\hbar}{2}\sum_{\vec{q}}(\vec{q}\cdot\vec{u}_0)\left\{[N_{\vec{q}}(\omega_{\rm LO})+1]\left\{\frac{\partial}{\partial\varepsilon_k}\right\}_{[n]}\Theta^{\rm em}_{\vec{k},\vec{q}}-N_{\vec{q}}(\omega_{\rm LO})\left\{\frac{\partial}{\partial\varepsilon_k}\right\}_{[n]}\Theta^{\rm abs}_{\vec{k},\vec{q}}\right\}+\mathcal{W}^{\rm (in)}_{\vec{k}}(1-n_{\vec{k}})-\mathcal{W}^{\rm (out)}_{\vec{k}}n_{\vec{k}},\end{aligned} \tag{10}$$

where $n_{\vec{k}}$ is the electron-distribution function in the k state, and the energy-drift term $-(\frac{1}{2})[\partial/\partial\varepsilon_k]_{[n]}\{(\vec{F}_{\rm i}[\vec{u}_0]+\vec{F}_{\rm p}[\vec{u}_0])\cdot\vec{u}_0\}$, due to the work done by the frictional force against the drift motion, has been included. The energy-drift term physically represents the rate for increasing the thermal energy of electrons in the $\vec{k}$ state. The work done by the frictional force was introduced in the energy-balance equation[3,8] to determine a macroscopic (state-independent) electron temperature. On the other hand, the work done by the frictional force is introduced here to microscopically determine the thermal effects on the electron distribution under high electric fields, without having to define an electron temperature, which is unphysical in the situation described here. The introduction of this additional term in Eq. (10) is crucial for the discussion of thermal effects on hot-electron trans-

port. In Eq. (10), $\{\partial/\partial\varepsilon_k\}_{[n]}$ indicates that the energy derivative only acts upon the occupation probability $n_{\vec{k}}$ or $n_{\vec{k}\pm\vec{q}}$, $\hbar\vec{q}\cdot\vec{u}_0$ is the Doppler shift in the energy of moving electrons along the field direction, $\hbar\omega_{q\lambda}$ is the energy of acoustic phonons in the λ mode with a wave vector $\vec{q}$, $\hbar\omega_{\mathrm{LO}}$ is the energy of the longitudinal-optical phonons, $U_i(q)=Z_c e^2/[\epsilon_0\epsilon_r(q^2+Q_s^2)\mathcal{V}]$ is the interaction between electrons and impurities, Z_c is the charge number of ionized donor atoms, $Q_s^2=(e^2/\epsilon_0\epsilon_r)(m^*/\pi^2\hbar^2)(3\pi^2\sigma_{3D})^{1/3}$ for static screening, and $\sigma_{3D}=N_e/\mathcal{V}$ is the electron concentration in the doped-host semiconductors. $N_{\vec{q}\lambda}(\omega_{q\lambda})$ is the nonequilibrium acoustic-phonon distribution which satisfies the following Boltzmann scattering equation for hot phonons:

$$\frac{dN_{\vec{q}\lambda}(\omega_{q\lambda})}{dt}=\Theta_{\vec{q}\lambda}^{\mathrm{em}}[N_{\vec{q}\lambda}(\omega_{q\lambda})+1]-\Theta_{\vec{q}\lambda}^{\mathrm{abs}}N_{\vec{q}\lambda}(\omega_{q\lambda})-\frac{N_{\vec{q}\lambda}(\omega_{q\lambda})-N_0(\hbar\omega_{q\lambda}/k_BT)}{\tau_{\vec{q}\lambda}},\tag{11}$$

where $\Theta_{\vec{q}\lambda}^{\mathrm{em}}$ and $\Theta_{\vec{q}\lambda}^{\mathrm{abs}}$ are the rates for acoustic-phonon emission and absorption, respectively, $\tau_{\vec{q}\lambda}$ is the relaxation time for acoustic phonons with wave vector $\vec{q}$ and in mode λ, $N_0(x)=[\exp(x)-1]^{-1}$ is the Bose-Einstein function, and T is the initial lattice temperature. For optical phonons, the nonequilibrium distribution $N_{\vec{q}}(\omega_{\mathrm{LO}})$ can be determined in a similar way by the following equation:

$$\frac{dN_{\vec{q}}(\omega_{\mathrm{LO}})}{dt}=\Theta_{\vec{q}}^{\mathrm{em}}[N_{\vec{q}}(\omega_{\mathrm{LO}})+1]-\Theta_{\vec{q}}^{\mathrm{abs}}N_{\vec{q}}(\omega_{\mathrm{LO}})-\frac{N_{\vec{q}}(\omega_{\mathrm{LO}})-N_0(\hbar\omega_{\mathrm{LO}}/k_BT)}{\tau_{\vec{q}}},\tag{12}$$

where $\Theta_{\vec{q}}^{\mathrm{em}}$ and $\Theta_{\vec{q}}^{\mathrm{abs}}$ are the rates for optical-phonon emission and absorption, respectively, and $\tau_{\vec{q}}$ is the relaxation time for optical phonons with wave vector $\vec{q}$. The lack of dependence of ω_{LO} on the wave number q will alter the momentum exchange between the electrons and the optical phonons during a scattering process. We have introduced a relaxation-time approximation in Eqs. (11) and (12) for additional phonon scattering other than the electron-phonon scattering. This additional phonon scattering includes both phonon-phonon interaction and boundary scattering of phonons.

The scattering-in rate for electrons in the final k state is

$$\begin{aligned}\mathcal{W}_{\vec{k}}^{(\mathrm{in})}=N_a\frac{2\pi}{\hbar}\sum_{\vec{q}}|U_i(q)|^2[n_{\vec{k}-\vec{q}}\delta(\varepsilon_k-\varepsilon_{k-q}+\hbar\vec{q}\cdot\vec{u}_0)+n_{\vec{k}+\vec{q}}\delta(\varepsilon_k-\varepsilon_{k+q}-\hbar\vec{q}\cdot\vec{u}_0)]+\frac{2\pi}{\hbar}\sum_{\vec{q},\lambda}|C_{q\lambda}|^2\{n_{\vec{k}-\vec{q}}N_{\vec{q}\lambda}(\omega_{q\lambda})\delta(\varepsilon_k-\varepsilon_{k-q}-\hbar\omega_{q\lambda}\\+\hbar\vec{q}\cdot\vec{u}_0)+n_{\vec{k}+\vec{q}}[N_{\vec{q}\lambda}(\omega_{q\lambda})+1]\delta(\varepsilon_k-\varepsilon_{k+q}+\hbar\omega_{q\lambda}-\hbar\vec{q}\cdot\vec{u}_0)\}+\frac{2\pi}{\hbar}\sum_{\vec{q}}|C_q|^2\{n_{\vec{k}-\vec{q}}N_{\vec{q}}(\omega_{\mathrm{LO}})\delta(\varepsilon_k-\varepsilon_{k-q}-\hbar\omega_{\mathrm{LO}}+\hbar\vec{q}\cdot\vec{u}_0)\\+n_{\vec{k}+\vec{q}}[N_{\vec{q}}(\omega_{\mathrm{LO}})+1]\delta(\varepsilon_k-\varepsilon_{k+q}+\hbar\omega_{\mathrm{LO}}-\hbar\vec{q}\cdot\vec{u}_0)\}+\frac{2\pi}{\hbar}\sum_{\vec{k}',\vec{q}}\left(\frac{e^2}{\epsilon_0\epsilon_r q^2\mathcal{V}}\right)^2(1-n_{\vec{k}'})n_{\vec{k}-\vec{q}}n_{\vec{k}'+\vec{q}}\delta(\varepsilon_k+\varepsilon_{k'}-\varepsilon_{k-q}-\varepsilon_{k'+q}),\end{aligned}\tag{13}$$

where the last term in Eq. (13) is due to Coulomb scattering, and the scattering-out rate for electrons in the initial k state is

$$\begin{aligned}\mathcal{W}_{\vec{k}}^{(\mathrm{out})}=N_a\frac{2\pi}{\hbar}\sum_{\vec{q}}|U_i(q)|^2[(1-n_{\vec{k}+\vec{q}})\delta(\varepsilon_{k+q}-\varepsilon_k+\hbar\vec{q}\cdot\vec{u}_0)+(1-n_{\vec{k}-\vec{q}})\delta(\varepsilon_{k-q}-\varepsilon_k-\hbar\vec{q}\cdot\vec{u}_0)]+\frac{2\pi}{\hbar}\sum_{\vec{q},\lambda}|C_{q\lambda}|^2\{(1-n_{\vec{k}+\vec{q}})\\\times N_{\vec{q}\lambda}(\omega_{q\lambda})\delta(\varepsilon_{k+q}-\varepsilon_k-\hbar\omega_{q\lambda}+\hbar\vec{q}\cdot\vec{u}_0)+(1-n_{\vec{k}-\vec{q}})[N_{\vec{q}\lambda}(\omega_{q\lambda})+1]\delta(\varepsilon_{k-q}-\varepsilon_k+\hbar\omega_{q\lambda}-\hbar\vec{q}\cdot\vec{u}_0)\}+\frac{2\pi}{\hbar}\sum_{\vec{q}}|C_q|^2\\\times\{(1-n_{\vec{k}+\vec{q}})N_{\vec{q}}(\omega_{\mathrm{LO}})\delta(\varepsilon_{k+q}-\varepsilon_k-\hbar\omega_{\mathrm{LO}}+\hbar\vec{q}\cdot\vec{u}_0)+(1-n_{\vec{k}-\vec{q}})[N_{\vec{q}}(\omega_{\mathrm{LO}})+1]\delta(\varepsilon_{k-q}-\varepsilon_k+\hbar\omega_{\mathrm{LO}}-\hbar\vec{q}\cdot\vec{u}_0)\}\\+\frac{2\pi}{\hbar}\sum_{\vec{k}',\vec{q}}\left(\frac{e^2}{\epsilon_0\epsilon_r q^2\mathcal{V}}\right)^2n_{\vec{k}'}(1-n_{\vec{k}-\vec{q}})(1-n_{\vec{k}'+\vec{q}})\delta(\varepsilon_{k-q}+\varepsilon_{k'+q}-\varepsilon_k-\varepsilon_{k'}).\end{aligned}\tag{14}$$

For the scattering-in rate, the first term in Eq. (13) is diagrammatically represented by the top panel in Fig. 1. The second and third terms in Eq. (13) are diagrammatically represented by the top panel in Fig. 2. On the other hand, the first term in Eq. (14) for the scattering-out rate is diagrammatically represented by the bottom panel in Fig. 1. The

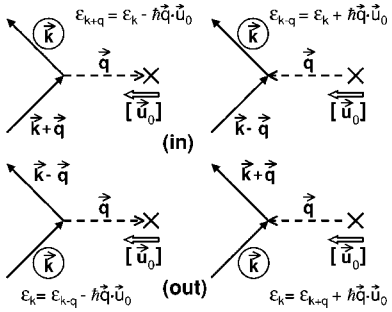

FIG. 1. Diagrams for scattering-in (top panel) and scattering-out (bottom panel) rates of moving electrons with static-impurity atoms. The solid lines with arrows represent the electron states with wave vectors indicated. The dashed lines with crosses represent the interactions of electrons with impurities with the wave vector $\vec{q}$. The circled wave vector $\vec{k}$ of electrons denotes the initial state for the scattering-out rate and the final state for the scattering-in rate. $\vec{u}_0$ is the electron drift velocity with its direction indicated by a hollow arrow in the dc-field direction. The conditions for energy conservation in each case are also shown among the electron kinetic energies ε_k and $\varepsilon_{k\pm q}$, and the Doppler shift $\hbar\vec{q}\cdot\vec{u}_0$.

second and third terms in Eq. (14) are diagrammatically represented by the bottom panel in Fig. 2.

The emission rate for acoustic phonons in the λ mode with a wave vector $\vec{q}$ due to the interaction of phonons with electrons is

$$\Theta^{\rm em}_{\vec{q}\lambda} \equiv \sum_{\vec{k}} \Theta^{\rm em}_{\vec{k},\vec{q}\lambda} = \frac{4\pi}{\hbar}|C_{q\lambda}|^2 \sum_{\vec{k}} \{n_{\vec{k}+\vec{q}}(1-n_{\vec{k}}) \times \delta(\varepsilon_k - \varepsilon_{k+q} + \hbar\omega_{q\lambda} - \hbar\vec{q}\cdot\vec{u}_0) + n_{\vec{k}}(1-n_{\vec{k}-\vec{q}})\delta(\varepsilon_{k-q} - \varepsilon_k + \hbar\omega_{q\lambda} - \hbar\vec{q}\cdot\vec{u}_0)\}, \tag{15}$$

and the absorption rate for acoustic phonons in the λ mode with a wave vector $\vec{q}$ is

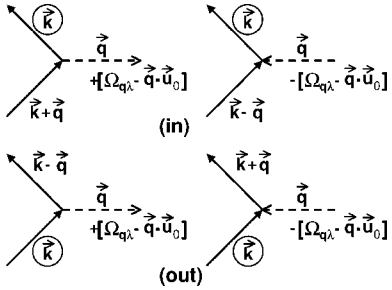

FIG. 2. Diagrams for scattering-in (top panel) and scattering-out (bottom panel) rates of moving electrons with static-lattice ions. The solid lines with arrows represent the electron states with wave vectors indicated. The dashed lines with arrows represent the interactions of carriers with phonons with the wave vector $\vec{q}$. The circled wave vector $\vec{k}$ of electrons denotes the initial state for the scattering-out rate and the final state for the scattering-in rate. $\Omega_{q\lambda}=\omega_{q\lambda}$ or $\omega_{\rm LO}$ denotes the phonon frequency and $\vec{q}\cdot\vec{u}_0$ is the Doppler shift.

$$\Theta^{\rm abs}_{\vec{q}\lambda} \equiv \sum_{\vec{k}} \Theta^{\rm abs}_{\vec{k},\vec{q}\lambda} = \frac{4\pi}{\hbar}|C_{q\lambda}|^2 \sum_{\vec{k}} \{n_{\vec{k}-\vec{q}}(1-n_{\vec{k}}) \times \delta(\varepsilon_k - \varepsilon_{k-q} - \hbar\omega_{q\lambda} + \hbar\vec{q}\cdot\vec{u}_0) + n_{\vec{k}}(1-n_{\vec{k}+\vec{q}})\delta(\varepsilon_{k+q} - \varepsilon_k - \hbar\omega_{q\lambda} + \hbar\vec{q}\cdot\vec{u}_0)\}. \tag{16}$$

For optical phonons, we have

$$\Theta^{\rm em}_{\vec{q}} \equiv \sum_{\vec{k}} \Theta^{\rm em}_{\vec{k},\vec{q}} = \frac{4\pi}{\hbar}|C_q|^2 \sum_{\vec{k}} \{n_{\vec{k}+\vec{q}}(1-n_{\vec{k}}) \times \delta(\varepsilon_k - \varepsilon_{k+q} + \hbar\omega_{\rm LO} - \hbar\vec{q}\cdot\vec{u}_0) + n_{\vec{k}}(1-n_{\vec{k}-\vec{q}})\delta(\varepsilon_{k-q} - \varepsilon_k + \hbar\omega_{\rm LO} - \hbar\vec{q}\cdot\vec{u}_0)\}, \tag{17}$$

and

$$\Theta^{\rm abs}_{\vec{q}} \equiv \sum_{\vec{k}} \Theta^{\rm abs}_{\vec{k},\vec{q}} = \frac{4\pi}{\hbar}|C_q|^2 \sum_{\vec{k}} \{n_{\vec{k}-\vec{q}}(1-n_{\vec{k}}) \times \delta(\varepsilon_k - \varepsilon_{k-q} - \hbar\omega_{\rm LO} + \hbar\vec{q}\cdot\vec{u}_0) + n_{\vec{k}}(1-n_{\vec{k}+\vec{q}})\delta(\varepsilon_{k+q} - \varepsilon_k - \hbar\omega_{\rm LO} + \hbar\vec{q}\cdot\vec{u}_0)\}. \tag{18}$$

For the phonon-emission rate in Eq. (15), its diagrammatical representation is shown by the top panel in Fig. 3. On the other hand, the diagrammatical representation of the phonon-absorption rate in Eq. (16) is displayed by the bottom panel in Fig. 3. In Eqs. (13)–(18), we have defined[9]

$$|C_{q\ell}|^2 = \frac{\hbar}{2\rho_{\rm i}\mathcal{V}\omega_{q\ell}}\left[D^2q^2 + \frac{9}{32}(eh_{14})^2\right]\left(\frac{q^2}{q^2+Q_s^2}\right)^2, \tag{19}$$

$$|C_{qt}|^2 = \frac{\hbar}{2\rho_{\rm i}\mathcal{V}\omega_{qt}}\frac{13}{64}(eh_{14})^2\left(\frac{q^2}{q^2+Q_s^2}\right)^2, \tag{20}$$

for the couplings between the electrons and the longitudinal ($\lambda=\ell$) and transverse ($\lambda=t$) acoustic phonons with $\omega_{q\lambda}=qs_\lambda$ in the Debye model, where s_λ is the sound velocity of acoustic phonons in the λ mode, $\rho_{\rm i}$ is the ion-mass density, D is the deformation potential, and h_{14} is the piezoelectric constant. For optical phonons, we have[1]

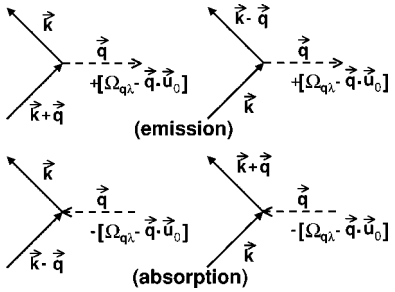

FIG. 3. Diagrams for phonon-emission (top panel) and phonon-absorption (bottom panel) rates due to interaction of moving electrons with static-lattice ions. The solid lines with arrows represent the electron states with wave vectors indicated. The dashed lines with arrows represent the interactions of carriers with phonons with the wave vector $\vec{q}$. $\Omega_{q\lambda}=\omega_{q\lambda}$ or $\omega_{\rm LO}$ denotes the phonon frequency and $\vec{q}\cdot\vec{u}_0$ is the Doppler shift.

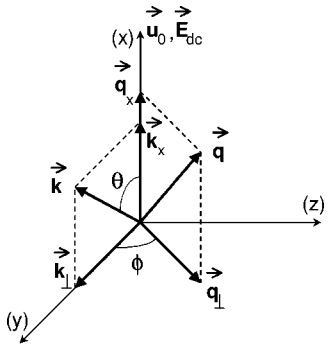

FIG. 4. Illustration for orientations of electron ($\vec{k}$) and phonon ($\vec{q}$) wave vectors. The applied electric field $\vec{E}_{\rm dc}$ and electron drift velocity $\vec{u}_0$ lie in the (x) direction. The electron wave vector $\vec{k}$ can be decomposed as a parallel component (k_x) (in the x direction) and a perpendicular component $\vec{k}_\perp$ (in the y direction due to rotational symmetry). The phonon wave vector $\vec{q}$ can also be decomposed in the same way. The angle between $\vec{q}_\perp$ and the y direction within the y-z plane is denoted by ϕ, and the angle between $\vec{k}$ and the x direction within the x-y plane is represented by θ.

$$|C_q|^2 = \frac{\hbar\omega_{\rm LO}}{2\mathcal{V}}\left(\frac{1}{\epsilon_\infty}-\frac{1}{\epsilon_s}\right)\frac{e^2}{\epsilon_0(q^2+Q_s^2)}, \tag{21}$$

where ϵ_s and ϵ_∞ are the static and high-frequency dielectric constants of host semiconductors.

By assuming a dc electric field along the x direction, as shown in Fig. 4, the force-balance equation for the center-of-mass motion of transported electrons is cast into the form of

$$N_e m^* \frac{du_0}{dt} = N_e e E_{\rm dc} + F_x[u_0], \tag{22}$$

where the quantum statistically averaged frictional force is found to be $F_x[u_0]=F_x^{\rm i}[u_0]+F_x^{\rm ph}[u_0]$ with[3,8]

$$F_x^{\rm i}[u_0] = -\frac{2\pi}{\hbar}\sum_{\vec{k},\vec{q}} \hbar q_x (n_{\vec{k}+\vec{q}} - n_{\vec{k}}) N_{\rm i} |U_{\rm i}(q)|^2 \times \delta(\varepsilon_{k+q} - \varepsilon_k + \hbar q_x u_0), \tag{23}$$

$$F_x^{\rm ph}[u_0] = -\sum_{\vec{k},\vec{q},\lambda} \hbar q_x \{\Theta^{\rm em}_{\vec{k},\vec{q}\lambda}[N_{\vec{q}\lambda}(\omega_{q\lambda})+1] - \Theta^{\rm abs}_{\vec{k},\vec{q}\lambda} N_{\vec{q}\lambda}(\omega_{q\lambda})\} - \sum_{\vec{k},\vec{q}} \hbar q_x \{\Theta^{\rm em}_{\vec{k},\vec{q}}[N_{\vec{q}}(\omega_{\rm LO})+1] - \Theta^{\rm abs}_{\vec{k},\vec{q}} N_{\vec{q}}(\omega_{\rm LO})\}. \tag{24}$$

$F_x^{\rm i}[u_0]$ and $F_x^{\rm ph}[u_0]$ are due to impurity and phonon scattering, respectively. Because of the Doppler shift in LO-phonon energy, i.e., $\omega_{\rm LO}-\hbar\vec{q}\cdot\vec{u}_0$ for phonon absorption and emission rates in Eqs. (17) and (18), the LO-phonon contribution to the frictional force in Eq. (24) becomes nonzero. In addition, Eq. (24) reduces to $-N_e m^* u_0/\tau_{\rm ph}$ in the leading order of small u_0 under a weak electric field, where $\tau_{\rm ph}$ can be viewed as a momentum-relaxation time of electrons from phonon scattering. The diagrammatical representation of $F_x^{\rm ph}[u_0]$ in Eq. (24) can be seen from Fig. 5 for the phonon-emission event (left panel) and the phonon-absorption event (right panel). The diagrammatical representation of $F_x^{\rm i}[u_0]$ in Eq. (23) can be found from Fig. 6.

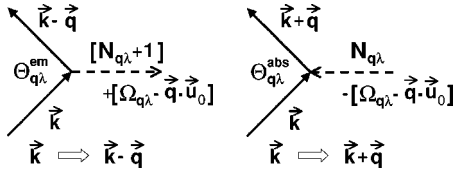

FIG. 5. Diagrams for changes of the electron momentum due to phonon emission (left panel) and phonon absorption (right panel). For each phonon-emission event with a rate $\Theta^{\rm em}_{q\lambda}$ and an occupation factor $N_{q\lambda}+1$, the electron wave number is reduced from the initial value k_x to the final value k_x-q_x in the field direction by the phonon wave number q_x, as indicated by a hollow arrow in the left panel. For each phonon-absorption event with a rate $\Theta^{\rm abs}_{q\lambda}$ and an occupation factor $N_{q\lambda}$, the electron wave number is increased from the initial value k_x to the final value k_x+q_x in the field direction by the phonon wave number q_x, as indicated by a hollow arrow in the right panel. The total change of the electron wave vector in the direction perpendicular to the field is zero, since the individual contributions cancel each other. $\Omega_{q\lambda}$ denotes the phonon frequency and $\vec{q}\cdot\vec{u}_0$ is the Doppler shift.

When $\varepsilon_k, \varepsilon_{k\pm q} \gg \hbar q_x u_0, \hbar\omega_{q\lambda}$ is assumed for high densities of electrons, we can expand the energy-drift equation up to the second order by introducing a continuous distribution function $f(\varepsilon_{k_\perp}, \varepsilon_{k_x}) \equiv \rho(\varepsilon_k) n_{\vec{k}} = [(2m^*)^{3/2}(\varepsilon_k)^{1/2}/(2\pi^2\hbar^3)] n_{\vec{k}}$, with $\varepsilon_k = \varepsilon_{k_\perp} + \varepsilon_{k_x}$, $\varepsilon_{k_\perp} = \hbar^2 k_\perp^2/2m^*$, $\varepsilon_{k_x} = \hbar^2 k_x^2/2m^*$, $\vec{k} = (k_x, \vec{k}_\perp)$, and $\vec{q} = (q_x, \vec{q}_\perp)$. When the acoustic-phonon frequency (dominant phonon modes at low temperatures) and the Doppler shift are smaller than the plasma frequency of electrons, the static-screening model can be justified. For steady-state electron transport, the Coulomb scattering effect can be approximated by a homogeneous level broadening related to the lifetimes of quasiparticles. By using the above assumptions, the energy-drift equation leads to the following linearized Fokker-Planck-type equation, with respect to the distribution function,

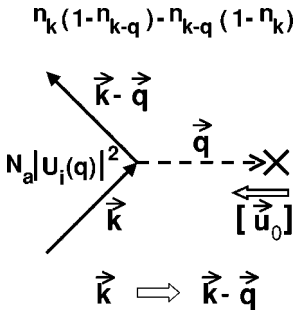

FIG. 6. Diagrams for changes of the electron momentum due to scattering with impurities. For each scattering event, the electron wave number is reduced from the initial value k_x to the final value k_x-q_x in the field direction by the wave number q_x of an impurity atom, as indicated by a hollow arrow at the bottom of the figure. $\vec{u}_0$ is the electron drift velocity with its direction indicated by a hollow arrow, and $N_a|U_{\rm i}(q)|^2$ represents the strength of impurity scattering. $n_{\vec{k}}(1-n_{\vec{k}-\vec{q}}) - n_{\vec{k}-\vec{q}}(1-n_{\vec{k}})$ represents the phase-space filling effect (Pauli exclusion) when the electron state $\vec{k}$ is the initial or final state in two opposite scattering events. The total change of the electron wave vector in the direction perpendicular to the field is zero, since the individual contributions cancel each other.

$$\frac{d}{dt}f(\varepsilon_{k_\perp},\varepsilon_{k_x}) = A_T(\varepsilon_{k_\perp},\varepsilon_{k_x})f(\varepsilon_{k_\perp},\varepsilon_{k_x}) - [V_T(\varepsilon_{k_\perp},\varepsilon_{k_x}) + V_F(\varepsilon_{k_\perp},\varepsilon_{k_x})]\left[\frac{\partial}{\partial\varepsilon_{k_\perp}} + \frac{\partial}{\partial\varepsilon_{k_x}}\right]f(\varepsilon_{k_\perp},\varepsilon_{k_x}) + [D_T(\varepsilon_{k_\perp},\varepsilon_{k_x}) + D_F(\varepsilon_{k_\perp},\varepsilon_{k_x})] \times \left[\frac{\partial^2}{\partial\varepsilon_{k_\perp}^2} + \frac{\partial^2}{\partial\varepsilon_{k_x}^2}\right]f(\varepsilon_{k_\perp},\varepsilon_{k_x}), \quad (25)$$

which is subjected to the conservation of the total number of electrons,

$$\sigma_{3D} = \frac{1}{2\pi^2}\int_0^{+\infty} dk_\perp k_\perp \int_{-\infty}^{+\infty} dk_x \left[\frac{f(\varepsilon_{k_\perp},\varepsilon_{k_x})}{\rho(\varepsilon_{k_\perp}+\varepsilon_{k_x})}\right]. \quad (26)$$

The spontaneous phonon-emission rate is

$$A_T(\varepsilon_{k_\perp},\varepsilon_{k_x}) = \frac{2\pi}{\hbar}\sum_{\vec{q},\lambda}|C_{q,\lambda}|^2[\delta(\varepsilon_k-\varepsilon_{k+q}+\hbar\omega_{q\lambda}-\hbar q_x u_0) - \delta(\varepsilon_k-\varepsilon_{k-q}-\hbar\omega_{q\lambda}+\hbar q_x u_0)] + \frac{2\pi}{\hbar}\sum_{\vec{q}}|C_q|^2[\delta(\varepsilon_k-\varepsilon_{k+q}+\hbar\omega_{LO}-\hbar q_x u_0) - \delta(\varepsilon_k-\varepsilon_{k-q}-\hbar\omega_{LO}+\hbar q_x u_0)]. \quad (27)$$

The thermal (T)-and dc-field (F)-induced energy transfer rates are

$$V_T(\varepsilon_{k_\perp},\varepsilon_{k_x}) = -2\pi N_i u_0\sum_{\vec{q}} q_x|U_i(q)|^2[\delta(\varepsilon_k-\varepsilon_{k-q}+\hbar q_x u_0) - \delta(\varepsilon_k-\varepsilon_{k+q}-\hbar q_x u_0)] + 2\pi\sum_{\vec{q},\lambda}(\omega_{q\lambda}-q_x u_0) \times|C_{q,\lambda}|^2\{N_{\vec{q}\lambda}(\omega_{q\lambda})\delta(\varepsilon_k-\varepsilon_{k-q}-\hbar\omega_{q\lambda}+\hbar q_x u_0) - [N_{\vec{q}\lambda}(\omega_{q\lambda})+1]\delta(\varepsilon_k-\varepsilon_{k+q}+\hbar\omega_{q\lambda}-\hbar q_x u_0)\} + 2\pi\sum_{\vec{q}}(\omega_{LO}-q_x u_0)|C_q|^2\{N_{\vec{q}}(\omega_{LO}) \times\delta(\varepsilon_k-\varepsilon_{k-q}-\hbar\omega_{LO}+\hbar q_x u_0) - [N_{\vec{q}}(\omega_{LO})+1] \times\delta(\varepsilon_k-\varepsilon_{k+q}+\hbar\omega_{LO}-\hbar q_x u_0)\}, \quad (28)$$

$$V_F(\varepsilon_{k_\perp},\varepsilon_{k_x}) = -2\pi u_0\sum_{\vec{q},\lambda} q_x|C_{q,\lambda}|^2[\delta(\varepsilon_k-\varepsilon_{k+q}+\hbar\omega_{q\lambda}-\hbar q_x u_0) + \delta(\varepsilon_{k-q}-\varepsilon_k+\hbar\omega_{q\lambda}-\hbar q_x u_0)] - 2\pi u_0\sum_{\vec{q}} q_x|C_q|^2[\delta(\varepsilon_k-\varepsilon_{k+q}+\hbar\omega_{LO}-\hbar q_x u_0) + \delta(\varepsilon_{k-q}-\varepsilon_k+\hbar\omega_{LO}-\hbar q_x u_0)]. \quad (29)$$

The thermal (T)-and dc-field (F)-induced energy-diffusion rates are

$$D_T(\varepsilon_{k_\perp},\varepsilon_{k_x}) = \pi N_i\hbar u_0^2\sum_{\vec{q}} q_x^2|U_i(q)|^2[\delta(\varepsilon_k-\varepsilon_{k-q}+\hbar q_x u_0) + \delta(\varepsilon_k-\varepsilon_{k+q}-\hbar q_x u_0)] + \pi\hbar\sum_{\vec{q},\lambda}(\omega_{q\lambda}-q_x u_0)^2|C_{q,\lambda}|^2\{N_{\vec{q}\lambda}(\omega_{q\lambda}) \times\delta(\varepsilon_k-\varepsilon_{k-q}-\hbar\omega_{q\lambda}+\hbar q_x u_0) + [N_{\vec{q}\lambda}(\omega_{q\lambda})+1] \times\delta(\varepsilon_k-\varepsilon_{k+q}+\hbar\omega_{q\lambda}-\hbar q_x u_0)\} + \pi\hbar\sum_{\vec{q}}(\omega_{LO}-q_x u_0)^2|C_q|^2\{N_{\vec{q}}(\omega_{LO}) \times\delta(\varepsilon_k-\varepsilon_{k-q}-\hbar\omega_{LO}+\hbar q_x u_0) + [N_{\vec{q}}(\omega_{LO})+1]\delta(\varepsilon_k-\varepsilon_{k+q}+\hbar\omega_{LO}-\hbar q_x u_0)\}, \quad (30)$$

$$D_F(\varepsilon_{k_\perp},\varepsilon_{k_x}) = -\pi N_i\hbar u_0^2\sum_{\vec{q}} q_x^2|U_i(q)|^2\delta(\varepsilon_{k+q}-\varepsilon_k+\hbar q_x u_0) - 2\pi\hbar u_0\sum_{\vec{q},\lambda} q_x|C_{q\lambda}|^2\{(q_x u_0-\omega_{q\lambda}) \times[N_{\vec{q}\lambda}(\omega_{q\lambda})+1]\delta(\varepsilon_k-\varepsilon_{k+q}+\hbar\omega_{q\lambda} - \hbar q_x u_0) - (q_x u_0+\omega_{q\lambda})N_{\vec{q}\lambda}(\omega_{q\lambda}) \times\delta(\varepsilon_k-\varepsilon_{k+q}-\hbar\omega_{q\lambda}-\hbar q_x u_0)\} - 2\pi\hbar u_0\sum_{\vec{q}} q_x|C_q|^2\{(q_x u_0-\omega_{LO}) \times[N_{\vec{q}}(\omega_{LO})+1]\delta(\varepsilon_k-\varepsilon_{k+q}+\hbar\omega_{LO}-\hbar q_x u_0) - (q_x u_0+\omega_{LO})N_{\vec{q}}(\omega_{LO}) \times\delta(\varepsilon_k-\varepsilon_{k+q}-\hbar\omega_{LO}-\hbar q_x u_0)\}. \quad (31)$$

Similar to the second-order expansion of the energy-drift equation, we can expand the frictional force up to the first order,

$$F_x[u_0] = 2\pi\hbar\sum_{\vec{k},\vec{q}}\frac{1}{\rho(\varepsilon_k)}N_i q_x^2 u_0|U_i(q)|^2\delta(\varepsilon_{k+q}-\varepsilon_k+\hbar q_x u_0) \times\left[\frac{\partial}{\partial\varepsilon_{k_\perp}}+\frac{\partial}{\partial\varepsilon_{k_x}}\right]f(\varepsilon_{k_\perp},\varepsilon_{k_x}) - 4\pi\sum_{\vec{q},\lambda} q_x|C_{q,\lambda}|^2\sum_{\vec{k}}\frac{f(\varepsilon_{k_\perp},\varepsilon_{k_x})}{\rho(\varepsilon_k)}[\delta(\varepsilon_k-\varepsilon_{k+q} + \hbar\omega_{q\lambda}-\hbar q_x u_0) + \delta(\varepsilon_{k-q}-\varepsilon_k+\hbar\omega_{q\lambda}-\hbar q_x u_0)] + 4\pi\hbar\sum_{\vec{q},\lambda} q_x|C_{q,\lambda}|^2\sum_{\vec{k}}\frac{1}{\rho(\varepsilon_k)}\{(q_x u_0-\omega_{q\lambda})[N_{\vec{q}\lambda}(\omega_{q\lambda}) + 1]\delta(\varepsilon_k-\varepsilon_{k+q}+\hbar\omega_{q\lambda}-\hbar q_x u_0) + (q_x u_0+\omega_{q\lambda})N_{\vec{q}\lambda}(\omega_{q\lambda}) \times\delta(\varepsilon_k-\varepsilon_{k+q}-\hbar\omega_{q\lambda}-\hbar q_x u_0)\}\left[\frac{\partial}{\partial\varepsilon_{k_\perp}} + \frac{\partial}{\partial\varepsilon_{k_x}}\right]f(\varepsilon_{k_\perp},\varepsilon_{k_x}) - 4\pi\sum_{\vec{q}} q_x|C_q|^2\sum_{\vec{k}}\frac{f(\varepsilon_{k_\perp},\varepsilon_{k_x})}{\rho(\varepsilon_k)} \times[\delta(\varepsilon_k-\varepsilon_{k+q}+\hbar\omega_{LO}-\hbar q_x u_0) + \delta(\varepsilon_{k-q}-\varepsilon_k+\hbar\omega_{LO} - \hbar q_x u_0)] + 4\pi\hbar\sum_{\vec{q}} q_x|C_q|^2\sum_{\vec{k}}\frac{1}{\rho(\varepsilon_k)}\{(q_x u_0-\omega_{LO})[N_{\vec{q}}(\omega_{LO}) + 1]\delta(\varepsilon_k-\varepsilon_{k+q}+\hbar\omega_{LO}-\hbar q_x u_0) + (q_x u_0+\omega_{LO})N_{\vec{q}}(\omega_{LO})\delta(\varepsilon_k-\varepsilon_{k+q}-\hbar\omega_{LO}-\hbar q_x u_0)\} \times\left[\frac{\partial}{\partial\varepsilon_{k_\perp}}+\frac{\partial}{\partial\varepsilon_{k_x}}\right]f(\varepsilon_{k_\perp},\varepsilon_{k_x}). \quad (32)$$

By using the same expansion technique, the emission and absorption rates of acoustic phonons can be rewritten as

$$\Theta_{\vec{q}\lambda}^{\mathrm{em}} = \frac{4\pi}{\hbar}|C_{q\lambda}|^2 \sum_{\vec{k}} \frac{f(\varepsilon_{k_\perp}, \varepsilon_{k_x})}{\rho(\varepsilon_k)} [\delta(\varepsilon_k - \varepsilon_{k+q} + \hbar\omega_{q\lambda} - \hbar q_x u_0) + \delta(\varepsilon_{k-q} - \varepsilon_k + \hbar\omega_{q\lambda} - \hbar q_x u_0)] + 4\pi|C_{q\lambda}|^2(\omega_{q\lambda} - q_x u_0) \times \sum_{\vec{k}} \frac{1}{\rho(\varepsilon_k)} \delta(\varepsilon_k - \varepsilon_{k+q} + \hbar\omega_{q\lambda} - \hbar q_x u_0) \times \left[\frac{\partial}{\partial \varepsilon_{k_\perp}} + \frac{\partial}{\partial \varepsilon_{k_x}}\right] f(\varepsilon_{k_\perp}, \varepsilon_{k_x}), \tag{33}$$

$$\Theta_{\vec{q}\lambda}^{\mathrm{abs}} = \frac{4\pi}{\hbar}|C_{q\lambda}|^2 \sum_{\vec{k}} \frac{f(\varepsilon_{k_\perp}, \varepsilon_{k_x})}{\rho(\varepsilon_k)} [\delta(\varepsilon_k - \varepsilon_{k-q} - \hbar\omega_{q\lambda} + \hbar q_x u_0) + \delta(\varepsilon_{k+q} - \varepsilon_k - \hbar\omega_{q\lambda} + \hbar q_x u_0)] - 4\pi|C_{q\lambda}|^2(\omega_{q\lambda} - q_x u_0) \times \sum_{\vec{k}} \frac{1}{\rho(\varepsilon_k)} \delta(\varepsilon_k - \varepsilon_{k-q} - \hbar\omega_{q\lambda} + \hbar q_x u_0) \times \left[\frac{\partial}{\partial \varepsilon_{k_\perp}} + \frac{\partial}{\partial \varepsilon_{k_x}}\right] f(\varepsilon_{k_\perp}, \varepsilon_{k_x}). \tag{34}$$

For optical phonons, we have similar results,

$$\Theta_{\vec{q}}^{\mathrm{em}} = \frac{4\pi}{\hbar}|C_q|^2 \sum_{\vec{k}} \frac{f(\varepsilon_{k_\perp}, \varepsilon_{k_x})}{\rho(\varepsilon_k)} [\delta(\varepsilon_k - \varepsilon_{k+q} + \hbar\omega_{\mathrm{LO}} - \hbar q_x u_0) + \delta(\varepsilon_{k-q} - \varepsilon_k + \hbar\omega_{\mathrm{LO}} - \hbar q_x u_0)] + 4\pi|C_q|^2(\omega_{\mathrm{LO}} - q_x u_0) \times \sum_{\vec{k}} \frac{1}{\rho(\varepsilon_k)} \delta(\varepsilon_k - \varepsilon_{k+q} + \hbar\omega_{\mathrm{LO}} - \hbar q_x u_0) \times \left[\frac{\partial}{\partial \varepsilon_{k_\perp}} + \frac{\partial}{\partial \varepsilon_{k_x}}\right] f(\varepsilon_{k_\perp}, \varepsilon_{k_x}), \tag{35}$$

$$\Theta_{\vec{q}}^{\mathrm{abs}} = \frac{4\pi}{\hbar}|C_q|^2 \sum_{\vec{k}} \frac{f(\varepsilon_{k_\perp}, \varepsilon_{k_x})}{\rho(\varepsilon_k)} [\delta(\varepsilon_k - \varepsilon_{k-q} - \hbar\omega_{\mathrm{LO}} + \hbar q_x u_0) + \delta(\varepsilon_{k+q} - \varepsilon_k - \hbar\omega_{\mathrm{LO}} + \hbar q_x u_0)] - 4\pi|C_q|^2(\omega_{\mathrm{LO}} - q_x u_0) \times \sum_{\vec{k}} \frac{1}{\rho(\varepsilon_k)} \delta(\varepsilon_k - \varepsilon_{k-q} - \hbar\omega_{\mathrm{LO}} + \hbar q_x u_0) \times \left[\frac{\partial}{\partial \varepsilon_{k_\perp}} + \frac{\partial}{\partial \varepsilon_{k_x}}\right] f(\varepsilon_{k_\perp}, \varepsilon_{k_x}). \tag{36}$$

By defining the following three dimensionless functions after the angle integration over ϕ,

$$\kappa^{\pm}(\{\bar{k}\}, \{\bar{q}\}) = \int_0^{2\pi} \frac{d\phi}{2\pi} \left\{ \frac{\bar{\gamma}_0/\pi}{\bar{\gamma}_0^2 + [\bar{q}_x^2 \pm 2\bar{k}_x\bar{q}_x + \bar{q}_\perp^2 \pm 2\bar{k}_\perp\bar{q}_\perp \cos\phi \pm 2\bar{q}_x\bar{u}_0]^2} \right\}, \tag{37}$$

$$\xi_\lambda^{\pm}(\{\bar{k}\}, \{\bar{q}\}) = \int_0^{2\pi} \frac{d\phi}{2\pi} \left\{ \frac{\bar{\gamma}_0/\pi}{\bar{\gamma}_0^2 + [\bar{q}_x^2 \pm 2\bar{k}_x\bar{q}_x + \bar{q}_\perp^2 \pm 2\bar{k}_\perp\bar{q}_\perp \cos\phi \pm 2(\bar{q}_x\bar{u}_0 - \bar{q}\bar{s}_\lambda)]^2} \right\}, \tag{38}$$

$$\psi^{\pm}(\{\bar{k}\}, \{\bar{q}\}) = \int_0^{2\pi} \frac{d\phi}{2\pi} \left\{ \frac{\bar{\gamma}_0/\pi}{\bar{\gamma}_0^2 + [\bar{q}_x^2 \pm 2\bar{k}_x\bar{q}_x + \bar{q}_\perp^2 \pm 2\bar{k}_\perp\bar{q}_\perp \cos\phi \pm 2(\bar{q}_x\bar{u}_0 - \bar{\Omega})]^2} \right\}, \tag{39}$$

where $\{\bar{k}\} = (\bar{k}_x, \bar{k}_\perp)$, $\bar{k}_\perp = k_\perp/k_f$, $\bar{k}_x = k_x/k_f$, $\bar{k} = (\bar{k}_\perp^2 + \bar{k}_x^2)^{1/2}$, $\{\bar{q}\} = (\bar{q}_x, \bar{q}_\perp)$, $\bar{q}_\perp = q_\perp/k_f$, $\bar{q}_x = q_x/k_f$, $\bar{q} = (\bar{q}_\perp^2 + \bar{q}_x^2)^{1/2}$, $\bar{u}_0 = m^* u_0/\hbar k_f$, $\bar{s}_\lambda = m^* s_\lambda/\hbar k_f$, $\bar{\Omega} = m^*\Omega_{\mathrm{LO}}/(\hbar k_f^2)$, $\bar{\gamma}_0 = \gamma_0/\varepsilon_f$, $k_f = (3\pi^2\sigma_{3\mathrm{D}})^{1/3}$, $\varepsilon_f = \hbar^2 k_f^2/2m^*$, and γ_0 is homogeneous level broadening due to Coulomb scattering, the Fokker-Planck-type equation can be cast into a dimensionless form,

$$\frac{d}{d\bar{t}}\bar{f}(\bar{\varepsilon}_{k_\perp}, \bar{\varepsilon}_{k_x}) = \bar{A}_{\mathrm{T}}(\bar{\varepsilon}_{k_\perp}, \bar{\varepsilon}_{k_x})\bar{f}(\bar{\varepsilon}_{k_\perp}, \bar{\varepsilon}_{k_x}) - [\bar{V}_{\mathrm{T}}(\bar{\varepsilon}_{k_\perp}, \bar{\varepsilon}_{k_x}) + \bar{V}_{\mathrm{F}}(\bar{\varepsilon}_{k_\perp}, \bar{\varepsilon}_{k_x})] \left[\frac{\partial}{\partial \bar{\varepsilon}_{k_\perp}} + \frac{\partial}{\partial \bar{\varepsilon}_{k_x}}\right] \bar{f}(\bar{\varepsilon}_{k_\perp}, \bar{\varepsilon}_{k_x}) + [\bar{D}_{\mathrm{T}}(\bar{\varepsilon}_{k_\perp}, \bar{\varepsilon}_{k_x}) + \bar{D}_{\mathrm{F}}(\bar{\varepsilon}_{k_\perp}, \bar{\varepsilon}_{k_x})] \times \left[\frac{\partial^2}{\partial \bar{\varepsilon}_{k_\perp}^2} + \frac{\partial^2}{\partial \bar{\varepsilon}_{k_x}^2}\right] \bar{f}(\bar{\varepsilon}_{k_\perp}, \bar{\varepsilon}_{k_x}), \tag{40}$$

which is subjected to the constraint [see Eq. (26)],

$$\int_0^{+\infty} d\bar{k}_\perp \bar{k}_\perp \int_{-\infty}^{+\infty} d\bar{k}_x (\bar{k}_\perp^2 + \bar{k}_x^2)^{-1/2} \bar{f}(\bar{\varepsilon}_{k_\perp}, \bar{\varepsilon}_{k_x}) = \frac{1}{3\pi^2}, \tag{41}$$

where $\bar{t} = \varepsilon_f t/\hbar$, $\bar{f}(\bar{\varepsilon}_{k_\perp}, \bar{\varepsilon}_{k_x}) = (\varepsilon_f/3\pi^2\sigma_{3\mathrm{D}}) f(\varepsilon_{k_\perp}, \varepsilon_{k_x}) = [(\bar{\varepsilon}_{k_\perp} + \bar{\varepsilon}_{k_x})^{1/2}/2\pi^2] n_{\bar{k}}$, $\bar{\varepsilon}_{k_\perp} = \varepsilon_{k_\perp}/\varepsilon_f$, $\bar{\varepsilon}_{k_x} = \varepsilon_{k_x}/\varepsilon_f$. The expansion coefficients in Eq. (40) can be found from Eqs. (A1)–(A5) in Appendix. In a similar fashion, we can also express the dynamical equation for hot phonons into a dimensionless form

$$\frac{dN_{\vec{q}\lambda}(2\overline{qs_\lambda})}{d\overline{t}} = \overline{\Theta}^{\rm em}_{\vec{q}\lambda}[N_{\vec{q}\lambda}(2\overline{qs_\lambda}) + 1] - \overline{\Theta}^{\rm abs}_{\vec{q}\lambda} N_{\vec{q}\lambda}(2\overline{qs_\lambda}) - \frac{N_{\vec{q}\lambda}(2\overline{qs_\lambda}) - N_0(2\overline{qs_\lambda}/\overline{T})}{\overline{\tau}_{\vec{q}\lambda}}, \tag{42}$$

$$\frac{dN_{\vec{q}}(2\overline{\Omega})}{d\overline{t}} = \overline{\Theta}^{\rm em}_{\vec{q}}[N_{\vec{q}}(2\overline{\Omega}) + 1] - \overline{\Theta}^{\rm abs}_{\vec{q}} N_{\vec{q}}(2\overline{\Omega}) - \frac{N_{\vec{q}\lambda}(2\overline{\Omega}) - N_0(2\overline{\Omega}/\overline{T})}{\overline{\tau}_{\vec{q}}}, \tag{43}$$

where $\overline{T}=k_{\rm B}T/\varepsilon_f$, $\overline{\tau}_{\vec{q}\lambda}=\varepsilon_f\tau_{\vec{q}\lambda}/\hbar$ and $\overline{\tau}_{\vec{q}}=\varepsilon_f\tau_{\vec{q}}/\hbar$. In Eqs. (42) and (43), the expansions for the dimensionless emission and absorption rates of phonons are given by Eqs. (A9)–(A12) in the Appendix. In addition, the force-balance equation can also be cast into a dimensionless form,

$$\frac{d\overline{u_0}}{d\overline{t}} = \overline{E}_{\rm dc} + \overline{F}_x[\overline{u_0}], \tag{44}$$

where $\overline{E}_{\rm dc}=eE_{\rm dc}/k_f\varepsilon_f$, and the dimensionless frictional force takes the form of

$$\begin{aligned}
\overline{F}_x[\overline{u_0}] \equiv \frac{F_x[u_0]}{N_e\varepsilon_f k_f} = \frac{n_{\rm i}\overline{u_0}}{2\pi\sigma_{\rm 3D}}\int_0^{+\infty} d\overline{k}_\perp \overline{k}_\perp \int_{-\infty}^{+\infty} d\overline{k}_x (\overline{k}_\perp^2 + \overline{k}_x^2)^{-1/2} \int_0^{+\infty} d\overline{q}_\perp \overline{q}_\perp \int_{-\infty}^{+\infty} d\overline{q}_x \overline{q}_x^2 |\overline{U}_{\rm i}(\overline{q})|^2 \kappa^+(\{\overline{k}\},\{\overline{q}\}) \left[\frac{\partial}{\partial\overline{\varepsilon}_{k_\perp}}\right. \\
\left. + \frac{\partial}{\partial\overline{\varepsilon}_{k_x}}\right]\overline{f}(\overline{\varepsilon}_{k_\perp},\overline{\varepsilon}_{k_x}) - \frac{3\pi}{2}\int_0^{+\infty} d\overline{k}_\perp \overline{k}_\perp \int_{-\infty}^{+\infty} d\overline{k}_x (\overline{k}_\perp^2 + \overline{k}_x^2)^{-1/2} \overline{f}(\overline{\varepsilon}_{k_\perp},\overline{\varepsilon}_{k_x}) \sum_\lambda \int_0^{+\infty} d\overline{q}_\perp \overline{q}_\perp \int_{-\infty}^{+\infty} d\overline{q}_x \overline{q}_x |\overline{C}_{\vec{q}\lambda}|^2 [\xi^{(+)}_\lambda(\{\overline{k}\},\{\overline{q}\}) \\
+ \xi^{(-)}_\lambda(\{\overline{k}\},\{\overline{q}\})] + 3\pi\int_0^{+\infty} d\overline{k}_\perp \overline{k}_\perp \int_{-\infty}^{+\infty} d\overline{k}_x (\overline{k}_\perp^2 + \overline{k}_x^2)^{-1/2} \sum_\lambda \int_0^{+\infty} d\overline{q}_\perp \overline{q}_\perp \int_{-\infty}^{+\infty} d\overline{q}_x \overline{q}_x (\overline{q}_x\overline{u}_0 - \overline{qs}_\lambda) |\overline{C}_{\vec{q}\lambda}|^2 \times \{[N_{\vec{q}\lambda}(2\overline{qs}_\lambda) \\
+ 1]\xi^{(+)}_\lambda(\{\overline{k}\},\{\overline{q}\}) + N_{\vec{q}\lambda}(2\overline{qs}_\lambda)\xi^{(-)}_\lambda(\{\overline{k}\},\{\overline{q}\})\}\left[\frac{\partial}{\partial\overline{\varepsilon}_{k_\perp}} + \frac{\partial}{\partial\overline{\varepsilon}_{k_x}}\right]\overline{f}(\overline{\varepsilon}_{k_\perp},\overline{\varepsilon}_{k_x}) - \frac{3\pi}{2}\int_0^{+\infty} d\overline{k}_\perp \overline{k}_\perp \int_{-\infty}^{+\infty} d\overline{k}_x (\overline{k}_\perp^2 \\
+ \overline{k}_x^2)^{-1/2} \overline{f}(\overline{\varepsilon}_{k_\perp},\overline{\varepsilon}_{k_x}) \int_0^{+\infty} d\overline{q}_\perp \overline{q}_\perp \int_{-\infty}^{+\infty} d\overline{q}_x \overline{q}_x |\overline{C}_{\vec{q}}|^2 [\psi^{(+)}(\{\overline{k}\},\{\overline{q}\}) + \psi^{(-)}(\{\overline{k}\},\{\overline{q}\})] + 3\pi\int_0^{+\infty} d\overline{k}_\perp \overline{k}_\perp \int_{-\infty}^{+\infty} d\overline{k}_x (\overline{k}_\perp^2 \\
+ \overline{k}_x^2)^{-1/2} \int_0^{+\infty} d\overline{q}_\perp \overline{q}_\perp \int_{-\infty}^{+\infty} d\overline{q}_x \overline{q}_x (\overline{q}_x\overline{u}_0 - \overline{\Omega}) |\overline{C}_{\vec{q}}|^2 \{[N_{\vec{q}}(2\overline{\Omega}) + 1]\psi^{(+)}(\{\overline{k}\},\{\overline{q}\}) + N_{\vec{q}}(2\overline{\Omega})\psi^{(-)}(\{\overline{k}\},\{\overline{q}\})\} \\
\times\left[\frac{\partial}{\partial\overline{\varepsilon}_{k_\perp}} + \frac{\partial}{\partial\overline{\varepsilon}_{k_x}}\right]\overline{f}(\overline{\varepsilon}_{k_\perp},\overline{\varepsilon}_{k_x}),
\end{aligned} \tag{45}$$

where $n_{\rm i}=N_{\rm a}/\mathcal{V}$, $|\overline{C}_{\vec{q}\lambda}|^2$, $|\overline{C}_{\vec{q}}|^2$ can be found from Eqs. (A6)–(A8) for $\lambda=t$, ℓ, and $|\overline{U}_{\rm i}(\overline{q})|^2$ can be found right below Eq. (A5).

III. NUMERICAL RESULTS

For our numerical calculations, we have chosen GaAs as an example for the host semiconductor. For GaAs, we have taken the following parameters: $\sigma_{\rm 3D}=1\times10^{18}$ cm^{-3}, $n_{\rm i}=1\times10^{15}$ cm^{-3}, $m^*/m_0=0.067$, $Z_c=1$, $\epsilon_s=13$, $\epsilon_\infty=11$, $\epsilon_r=12$, $s_\ell=5.14\times10^5$ cm/s, $s_t=3.04\times10^5$ cm/s, $D=-9.3$ eV, $h_{14}=1.2\times10^7$ V/cm, $\rho_i=5.3$ g/cm^3, $\gamma_0=5$ meV and $\tau_{\vec{q}\ell}=\tau_{\vec{q}t}=\tau_{\vec{q}}=3.5$ ps. The other parameters, lattice temperature T and electric field $E_{\rm dc}$, will be given in the figure captions. The electric field is assumed to be in the x direction.

Figure 7 displays the time evolution of the calculated drift velocity u_0 as it gradually reaches a steady state. This time-evolution method has been used previously[8] to seek a stable steady-state solution. In this case, the dc field is turned on right after $t=0$. From Fig. 7, the steady state is reached with u_0 on the order of 10^7 cm/s after $t>1.2$ ps, when $T=30$ K and $E_{\rm dc}=0.75$ kV/cm.

In order to elucidate the physics, we show the calculated distribution functions of electrons $(\varepsilon_f/k_f^3)f(\varepsilon_{k_\perp},\varepsilon_{k_x})$ in Fig. 8 at $T=30$ K and $E_{\rm dc}=0.75$ kV/cm as functions of $\varepsilon_{k_x}/\varepsilon_f$ with $k_\perp=0$ in Fig. 8(a) and $\varepsilon_{k_\perp}/\varepsilon_f$ with $k_x=0$ in Fig. 8(b). For the purpose of comparison, the equilibrium Fermi-Dirac distribution function is also shown in Fig. 8 by the dashed-dotted curve with the symbol □. From Fig. 8(a) it is easy to see that electrons are moved from $k_x>0$ states (dashed curve with the symbol △) to $k_x<0$ states (solid curve with the symbol

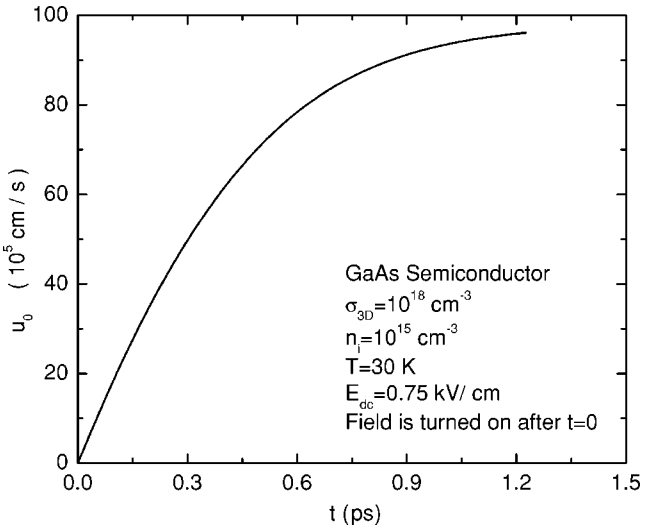

FIG. 7. Time evolution of calculated drift velocity u_0 as a function of time t at $T=30$ K and $E_{dc}=0.75$ kV/cm for hot electrons. The dc field is turned on right after $t=0$. u_0 linearly increases with t initially, and a steady state is finally reached after $t>1.2$ ps.

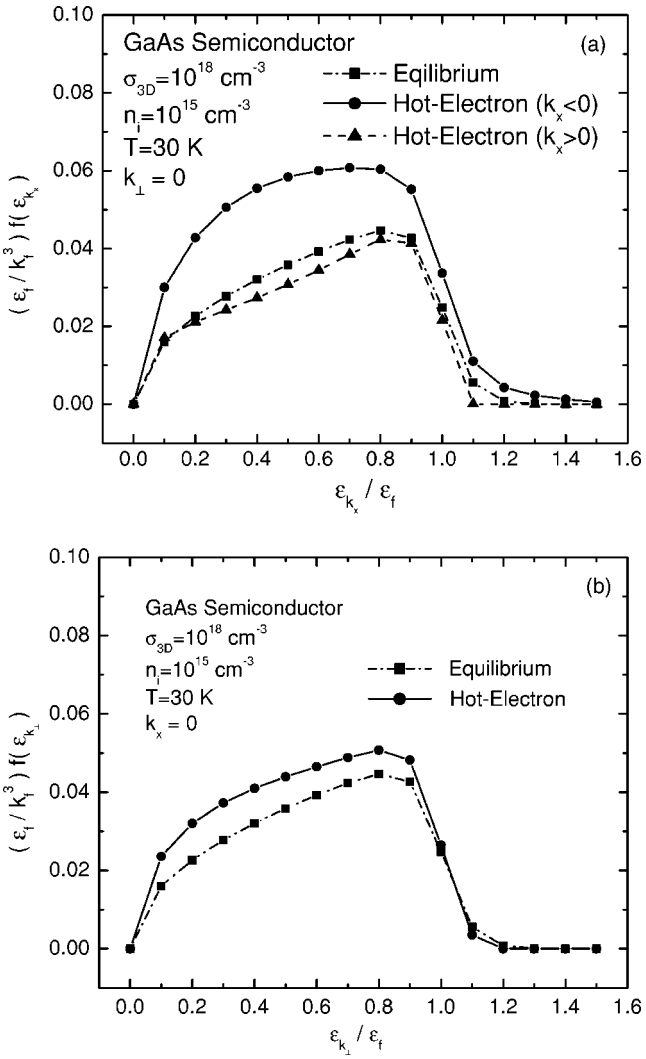

FIG. 8. Comparison of calculated dimensionless electron-distribution functions $\overline{f}(\overline{\varepsilon_{k_\perp}},\overline{\varepsilon_{k_x}})=(\varepsilon_f/3\pi^2\sigma_{3D})f(\varepsilon_{k_\perp},\varepsilon_{k_x})$ as functions of $\overline{\varepsilon_{k_x}}=\varepsilon_{k_x}/\varepsilon_f$ and $\overline{\varepsilon_{k_\perp}}=\varepsilon_{k_\perp}/\varepsilon_f$ in (a) and (b) at $T=30$ K and $E_{dc}=0.75$ kV/cm for hot and equilibrium electrons. The dashed-dotted curves in both (a) and (b) with the symbol □ represent the results from the equilibrium electrons. In (a), $k_\perp=0$ and the solid and dashed curves with symbols ○ and △ represent the results from the hot electrons with $k_x<0$ and $k_x>0$, respectively. In (b), $k_x=0$, and the solid curve with the symbol ○ represents the result from the hot electrons.

○) in the field direction, which is in sharp contrast with the assumption of an isotropic distribution of electrons in the momentum space adopted by the energy-balance equation.[3] Relatively cool electrons in $k_x>0$ states (sharp tail at the Fermi surface) are found in comparison with hot electrons in $k_x<0$ states (smooth tail at the Fermi surface). Moreover, we see by comparing Fig. 8(b) with Fig. 8(a) that the dependence of $f(\varepsilon_{k_\perp},\varepsilon_{k_x})$ on $k_\perp$ and k_x is also anisotropic, and the electrons are relatively unheated or cooled (almost identical Fermi surface) by the dc field in the direction perpendicular to the field. This excludes the possibility of defining a state-independent electron temperature as introduced by the energy-balance equation.[3]

Figure 9 illustrates the field dependence of calculated drift velocity u_0 in Fig. 9(a) and mobility $\mu_c=u_0/E_{dc}$ in Fig. 9(b) at $T=30$ K when the energy-drift term in Eq. (10) is included (solid curves with the symbol □) and excluded (dashed-dotted curves with the symbol ○). In Fig. 9(a) we can see that the energy-drift effect heats the electrons in the field direction and reduces the drift velocity when E_{dc} is strong (greater than 0.75 kV/cm). The nonlinear relation between the drift velocity and the applied dc field (solid curve) can be seen very clearly in the strong-field regime when the energy-drift effect is included, which is an indication of the high-field transport of hot electrons. Moreover, we find in Fig. 9(b) that the mobility μ_c decreases with E_{dc}, which has been observed previously from numerical calculations,[10] and the energy-drift effect further reduces the mobility when E_{dc} is higher than 0.75 kV/cm.

Finally, we conclude from Figs. 8 and 9 that the energy-drift equation derived in this work does include the additional hot-electron effect in the high-field transport in comparison with the regular Boltzmann transport equation. Furthermore, the energy-drift equation also includes the anisotropic distribution of electrons in momentum space along and perpendicular to the field direction, due to the acceleration of electrons by the dc electric field. This implies that the isotropic assumption adopted by the energy-balance equation cannot be justified under a strong dc electric field. On the other hand, when the dc field is weak, our coupled energy-drift and force-balance equations reduce to the same results as those obtained from coupled energy-balance and force-balance equations, as well as from the regular Boltzmann transport equation, when only the linear-field terms are kept.[3,4]

IV. CONCLUSIONS AND REMARKS

In conclusion, coupled energy-drift and force-balance equations have been derived for high-field hot-electron trans-

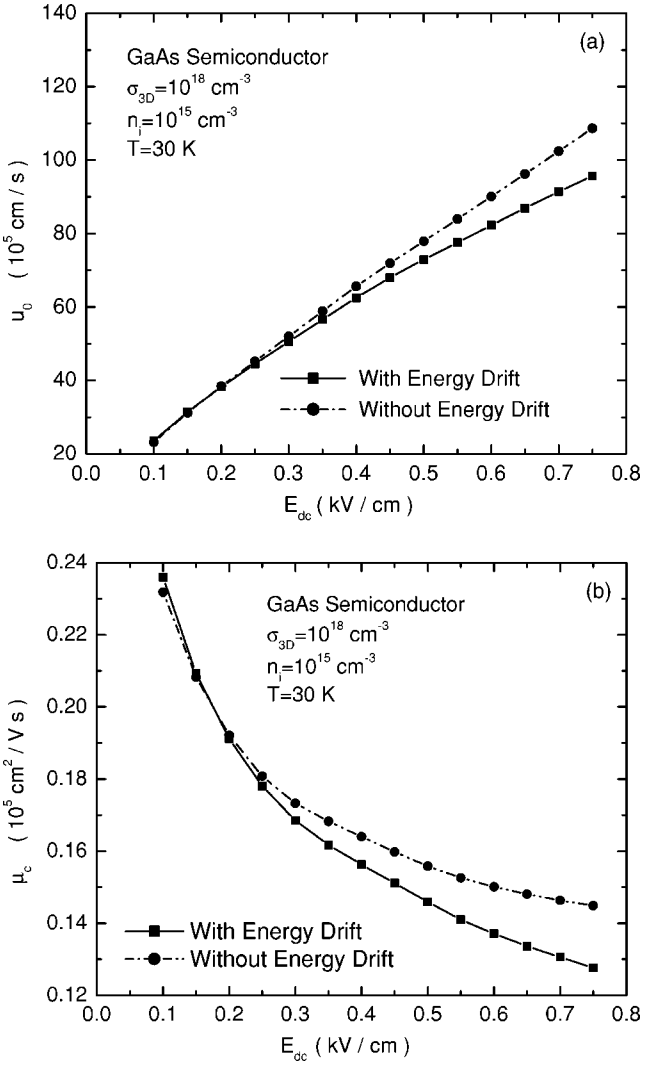

FIG. 9. Comparison of calculated drift velocities u_0 and mobilities $\mu_c=u_0/E_{dc}$ as functions of the electric field E_{dc} in (a) and (b) at $T=30$ K with (solid curves with the symbol □) and without (dashed curves with the symbol ○) an energy-drift term in the energy-drift equation.

port. The work done by the frictional force has been included in the Boltzmann scattering equation for electron relative-scattering motion and has been found to increase the thermal energy of the electrons and to reduce the field-dependent drift velocity and mobility of the electrons. The importance of the hot-electron effect in the energy-drift term under a strong dc field has been demonstrated. The Doppler shift in the energy conservation of scattering electrons interacting with impurities and phonons has been found to give rise to the anisotropic electron distribution in momentum space along the field direction. The importance of this anisotropic distribution has been demonstrated through a comparison with the isotropic energy-balance equation, from which the possibility for defining a state-independent electron temperature has been excluded.

The proposed energy-drift and force-balance equations can provide new physical insight in several areas. These include the study of current-injected hot-carrier energy relaxation in light-emitting diodes or quantum-well lasers,[11] the study of saturation drift velocities in different semiconductors,[12] the study of phonon-drag thermoelectric power,[9] and the study of the nonresonant interaction of carriers with terahertz radiation.[13]

By further incorporating the electric and magnetic potentials into the proposed energy-drift and force-balance equations, we will be able to explain nonlinear miniband transport in superlattices[14] and the magneto-transport effect in a two-dimensional electron gas (2DEG).[15] Moreover, by including the energy-drift term in the semiconductor Bloch equations,[7] we will be able to explain transport effects on laser-induced optical coherence and vice versa.

ACKNOWLEDGMENTS

The authors are grateful to Professor S. W. Koch and Professor J. V. Moloney for their helpful discussions on the relative scattering motion of electrons, and to Professor D. K. Ferry and Professor S. M. Goodnick for their helpful discussions on the dynamics of hot phonons. The authors are also grateful to Professor H. L. Cui for his helpful discussions and comments on the frictional force exerted on electrons from hot-phonon scattering. This research was supported by the Air Force Office of Scientific Research (AFOSR).

APPENDIX

By using the three dimensionless functions defined in Eqs. (37)–(39), we can express all the dimensionless expansion coefficients of the Fokker-Planck-type equation as

$$\overline{A}_T(\overline{\varepsilon}_{k_\perp},\overline{\varepsilon}_{k_x}) \equiv \frac{\hbar A_T(\varepsilon_{k_\perp},\varepsilon_{k_x})}{\varepsilon_f} = \frac{1}{2\pi}\sum_\lambda \int_0^{+\infty} d\overline{q}_\perp \overline{q}_\perp \times \int_{-\infty}^{+\infty} d\overline{q}_x |\overline{C}_{\overline{q}\lambda}|^2 [\xi_\lambda^+(\{\overline{k}\},\{\overline{q}\}) - \xi_\lambda^-(\{\overline{k}\},\{\overline{q}\})] + \frac{1}{2\pi}\int_0^{+\infty} d\overline{q}_\perp \overline{q}_\perp \int_{-\infty}^{+\infty} d\overline{q}_x |\overline{C}_{\overline{q}}|^2 [\psi^+(\{\overline{k}\},\{\overline{q}\}) - \psi^-(\{\overline{k}\},\{\overline{q}\})], \quad \text{(A1)}$$

$$\overline{V}_T(\overline{\varepsilon}_{k_\perp},\overline{\varepsilon}_{k_x}) \equiv \frac{\hbar V_T(\varepsilon_{k_\perp},\varepsilon_{k_x})}{\varepsilon_f^2} = -\left(\frac{n_i \overline{u}_0}{3\pi^3 \sigma_{3D}}\right)\int_0^{+\infty} d\overline{q}_\perp \overline{q}_\perp \int_{-\infty}^{+\infty} d\overline{q}_x \times \overline{q}_x |\overline{U}_i(\overline{q})|^2 [\kappa^-(\{\overline{k}\},\{\overline{q}\}) - \kappa^+(\{\overline{k}\},\{\overline{q}\})] - \frac{1}{\pi}\sum_\lambda \int_0^{+\infty} d\overline{q}_\perp \overline{q}_\perp \int_{-\infty}^{+\infty} d\overline{q}_x (\overline{q}_x \overline{u}_0 - \overline{q}\overline{s}_\lambda) |\overline{C}_{\overline{q}\lambda}|^2 \times \{N_{\overline{q}\lambda}(2\overline{q}\overline{s}_\lambda)\xi_\lambda^-(\{\overline{k}\},\{\overline{q}\}) - [N_{\overline{q}\lambda}(2\overline{q}\overline{s}_\lambda) + 1]\xi_\lambda^+(\{\overline{k}\},\{\overline{q}\})\} - \frac{1}{\pi}\int_0^{+\infty} d\overline{q}_\perp \overline{q}_\perp$$

$$\times \int_{-\infty}^{+\infty} d\bar{q}_x (\bar{q}_x \bar{u}_0 - \bar{\Omega}) |\bar{C}_{\vec{q}}|^2 \{ N_{\vec{q}}(2\bar{\Omega}) \psi^-(\{\bar{k}\},\{\bar{q}\}) - [N_{\vec{q}}(2\bar{\Omega}) + 1] \psi^+(\{\bar{k}\},\{\bar{q}\}) \}, \tag{A2}$$

$$\bar{V}_{\mathrm{F}}(\bar{\varepsilon}_{k_\perp}, \bar{\varepsilon}_{k_x}) \equiv \frac{\hbar V_{\mathrm{F}}(\varepsilon_{k_\perp}, \varepsilon_{k_x})}{\varepsilon_f^2} = -\frac{u_0}{\pi} \sum_\lambda \int_0^{+\infty} d\bar{q}_\perp \bar{q}_\perp \int_{-\infty}^{+\infty} d\bar{q}_x \bar{q}_x |\bar{C}_{\vec{q}\lambda}|^2 \times [\xi_\lambda^+(\{\bar{k}\},\{\bar{q}\}) + \xi_\lambda^-(\{\bar{k}\},\{\bar{q}\})] - \frac{u_0}{\pi} \int_0^{+\infty} d\bar{q}_\perp \bar{q}_\perp \int_{-\infty}^{+\infty} d\bar{q}_x \bar{q}_x |\bar{C}_{\vec{q}}|^2 [\psi^+(\{\bar{k}\},\{\bar{q}\}) + \psi^-(\{\bar{k}\},\{\bar{q}\})], \tag{A3}$$

$$\bar{D}_{\mathrm{T}}(\bar{\varepsilon}_{k_\perp}, \bar{\varepsilon}_{k_x}) \equiv \frac{\hbar D_{\mathrm{T}}(\varepsilon_{k_\perp}, \varepsilon_{k_x})}{\varepsilon_f^3} = \left(\frac{n_{\mathrm{i}} \bar{u}_0^2}{3\pi^3 \sigma_{3\mathrm{D}}} \right) \int_0^{+\infty} d\bar{q}_\perp \bar{q}_\perp \int_{-\infty}^{+\infty} d\bar{q}_x \times \bar{q}_x^2 |\bar{U}_{\mathrm{i}}(\bar{q})|^2 [\kappa^-(\{\bar{k}\},\{\bar{q}\}) + \kappa^+(\{\bar{k}\},\{\bar{q}\})] + \frac{1}{\pi} \sum_\lambda \int_0^{+\infty} d\bar{q}_\perp \bar{q}_\perp \int_{-\infty}^{+\infty} d\bar{q}_x (\bar{q}_x \bar{u}_0 - \bar{q}\bar{s}_\lambda)^2 |\bar{C}_{\vec{q}\lambda}|^2 \times \{ N_{\vec{q}\lambda}(2\bar{q}\bar{s}_\lambda) \xi_\lambda^-(\{\bar{k}\},\{\bar{q}\}) + [N_{\vec{q}\lambda}(2\bar{q}\bar{s}_\lambda) + 1] \xi_\lambda^+(\{\bar{k}\},\{\bar{q}\}) \} + \frac{1}{\pi} \int_0^{+\infty} d\bar{q}_\perp \bar{q}_\perp \int_{-\infty}^{+\infty} d\bar{q}_x (\bar{q}_x \bar{u}_0 - \bar{\Omega})^2 |\bar{C}_{\vec{q}}|^2 \times \{ N_{\vec{q}}(2\bar{\Omega}) \psi^-(\{\bar{k}\},\{\bar{q}\}) + [N_{\vec{q}}(2\bar{\Omega}) + 1] \psi^+(\{\bar{k}\},\{\bar{q}\}) \}, \tag{A4}$$

$$\bar{D}_{\mathrm{F}}(\bar{\varepsilon}_{k_\perp}, \bar{\varepsilon}_{k_x}) \equiv \frac{\hbar D_{\mathrm{E}}(\varepsilon_{k_\perp}, \varepsilon_{k_x})}{\varepsilon_f^3} = -\left(\frac{n_{\mathrm{i}} \bar{u}_0^2}{3\pi^3 \sigma_{3\mathrm{D}}} \right) \times \int_0^{+\infty} d\bar{q}_\perp \bar{q}_\perp \int_{-\infty}^{+\infty} d\bar{q}_x \bar{q}_x^2 |\bar{U}_{\mathrm{i}}(\bar{q})|^2 \kappa^+(\{\bar{k}\},\{\bar{q}\}) - \frac{2\bar{u}_0}{\pi} \sum_\lambda \int_0^{+\infty} d\bar{q}_\perp \bar{q}_\perp \times \int_{-\infty}^{+\infty} d\bar{q}_x \bar{q}_x (\bar{q}_x \bar{u}_0 - \bar{q}\bar{s}_\lambda) |\bar{C}_{\vec{q}\lambda}|^2 \times \{ [N_{\vec{q}\lambda}(2\bar{q}\bar{s}_\lambda) + 1] \xi_\lambda^+(\{\bar{k}\},\{\bar{q}\}) + N_{\vec{q}\lambda}(2\bar{q}\bar{s}_\lambda) \xi_\lambda^-(\{\bar{k}\},\{\bar{q}\}) \} - \frac{2\bar{u}_0}{\pi} \int_0^{+\infty} d\bar{q}_\perp \bar{q}_\perp \int_{-\infty}^{+\infty} d\bar{q}_x \bar{q}_x (\bar{q}_x \bar{u}_0 - \bar{\Omega}) |\bar{C}_{\vec{q}}|^2 \times \{ [N_{\vec{q}}(2\bar{\Omega}) + 1] \psi^+(\{\bar{k}\},\{\bar{q}\}) + N_{\vec{q}}(2\bar{\Omega}) \psi^-(\{\bar{k}\},\{\bar{q}\}) \}, \tag{A5}$$

where $n_{\mathrm{i}} = N_a / \mathcal{V}$ is the concentration of impurity atoms, $\bar{\varepsilon}_{k_\perp} = \varepsilon_{k_\perp} / \varepsilon_f$, $\bar{\varepsilon}_{k_x} = \varepsilon_{k_x} / \varepsilon_f$, $\bar{U}_{\mathrm{i}}(\bar{q}) = (Ze^2 k_f / \epsilon_0 \epsilon_r \varepsilon_f) / (\bar{q}_\perp^2 + \bar{q}_x^2 + \bar{Q}_s^2)$, $\bar{Q}_s^2 = (e^2 k_f / \epsilon_0 \epsilon_r \varepsilon_f) / (2\pi^2)$. Moreover, we find the dimensionless form for the electron-phonon coupling,

$$|\bar{C}_q|^2 = \frac{e^2 k_f \bar{\Omega}}{\epsilon_0 \varepsilon_f} \left(\frac{1}{\epsilon_\infty} - \frac{1}{\epsilon_s} \right) \frac{1}{\bar{q}_\perp^2 + \bar{q}_x^2 + \bar{Q}_s^2}, \tag{A6}$$

$$|\bar{C}_{\vec{q}\ell}|^2 = \left(\frac{m^* k_f^3}{2\rho_{\mathrm{i}} \bar{s}_\ell} \right) \left[\bar{D}^2 (\bar{q}_\perp^2 + \bar{q}_x^2) + \frac{9}{32} (e\bar{h}_{14})^2 \right] \frac{(\bar{q}_\perp^2 + \bar{q}_x^2)^{3/2}}{(\bar{q}_\perp^2 + \bar{q}_x^2 + \bar{Q}_s^2)^2}, \tag{A7}$$

$$|\bar{C}_{\vec{q}t}|^2 = \left(\frac{m^* k_f^3}{2\rho_{\mathrm{i}} \bar{s}_t} \right) \frac{13}{64} (e\bar{h}_{14})^2 \frac{(\bar{q}_\perp^2 + \bar{q}_x^2)^{3/2}}{(\bar{q}_\perp^2 + \bar{q}_x^2 + \bar{Q}_s^2)^2}, \tag{A8}$$

where $\bar{D} = D / \varepsilon_f$, $e\bar{h}_{14} = eh_{14} / k_f \varepsilon_f$.

By using the dimensionless functions defined in Eqs. (37)–(39), we can express all the dimensionless emission and absorption rates of the dynamical equation for hot phonons as

$$\bar{\Theta}_{\vec{q}\lambda}^{\mathrm{em}} \equiv \frac{\hbar \Theta_{\vec{q}\lambda}^{\mathrm{em}}}{\varepsilon_f} = 2\pi |\bar{C}_{\vec{q}\lambda}|^2 \int_0^{+\infty} d\bar{k}_\perp \bar{k}_\perp \int_{-\infty}^{+\infty} d\bar{k}_x (\bar{k}_\perp^2 + \bar{k}_x^2)^{-1/2} \times [\xi_\lambda^+(\{\bar{k}\},\{\bar{q}\}) + \xi_\lambda^-(\{\bar{k}\},\{\bar{q}\})] + 4\pi |\bar{C}_{\vec{q}\lambda}|^2 (\bar{q}\bar{s}_\lambda - \bar{q}_x \bar{u}_0) \times \int_0^{+\infty} d\bar{k}_\perp \bar{k}_\perp \int_{-\infty}^{+\infty} d\bar{k}_x (\bar{k}_\perp^2 + \bar{k}_x^2)^{-1/2} \xi_\lambda^+(\{\bar{k}\},\{\bar{q}\}) \times \left[\frac{\partial}{\partial \bar{\varepsilon}_{k_\perp}} + \frac{\partial}{\partial \bar{\varepsilon}_{k_x}} \right] \bar{f}(\bar{\varepsilon}_{k_\perp}, \bar{\varepsilon}_{k_x}), \tag{A9}$$

$$\bar{\Theta}_{\vec{q}\lambda}^{\mathrm{abs}} \equiv \frac{\hbar \Theta_{\vec{q}\lambda}^{\mathrm{abs}}}{\varepsilon_f} = 2\pi |\bar{C}_{\vec{q}\lambda}|^2 \int_0^{+\infty} d\bar{k}_\perp \bar{k}_\perp \int_{-\infty}^{+\infty} d\bar{k}_x (\bar{k}_\perp^2 + \bar{k}_x^2)^{-1/2} \times [\xi_\lambda^+(\{\bar{k}\},\{\bar{q}\}) + \xi_\lambda^-(\{\bar{k}\},\{\bar{q}\})] - 4\pi |\bar{C}_{\vec{q}\lambda}|^2 (\bar{q}\bar{s}_\lambda - \bar{q}_x \bar{u}_0) \times \int_0^{+\infty} d\bar{k}_\perp \bar{k}_\perp \int_{-\infty}^{+\infty} d\bar{k}_x (\bar{k}_\perp^2 + \bar{k}_x^2)^{-1/2} \xi_\lambda^-(\{\bar{k}\},\{\bar{q}\}) \times \left[\frac{\partial}{\partial \bar{\varepsilon}_{k_\perp}} + \frac{\partial}{\partial \bar{\varepsilon}_{k_x}} \right] \bar{f}(\bar{\varepsilon}_{k_\perp}, \bar{\varepsilon}_{k_x}). \tag{A10}$$

For optical phonons, we have similar results,

$$\bar{\Theta}^{\mathrm{em}}_{\vec{q}} \equiv \frac{\hbar\Theta^{\mathrm{em}}_{\vec{q}}}{\varepsilon_f} = 2\pi|\bar{C}_{\bar{q}}|^2 \int_0^{+\infty} d\bar{k}_\perp \bar{k}_\perp \int_{-\infty}^{+\infty} d\bar{k}_x (\bar{k}_\perp^2 + \bar{k}_x^2)^{-1/2}$$
$$\times [\psi^+(\{\bar{k}\},\{\bar{q}\}) + \psi^-(\{\bar{k}\},\{\bar{q}\})] + 4\pi|\bar{C}_{\bar{q}}|^2(\bar{\Omega} - \bar{q}_x\bar{u}_0)$$
$$\times \int_0^{+\infty} d\bar{k}_\perp \bar{k}_\perp \int_{-\infty}^{+\infty} d\bar{k}_x (\bar{k}_\perp^2 + \bar{k}_x^2)^{-1/2} \psi^+(\{\bar{k}\},\{\bar{q}\})$$
$$\times \left[\frac{\partial}{\partial \bar{\varepsilon}_{k_\perp}} + \frac{\partial}{\partial \bar{\varepsilon}_{k_x}}\right] \bar{f}(\bar{\varepsilon}_{k_\perp}, \bar{\varepsilon}_{k_x}), \tag{A11}$$

$$\bar{\Theta}^{\mathrm{abs}}_{\vec{q}} \equiv \frac{\hbar\Theta^{\mathrm{abs}}_{\vec{q}}}{\varepsilon_f} = 2\pi|\bar{C}_{\bar{q}}|^2 \int_0^{+\infty} d\bar{k}_\perp \bar{k}_\perp \int_{-\infty}^{+\infty} d\bar{k}_x (\bar{k}_\perp^2 + \bar{k}_x^2)^{-1/2}$$
$$\times [\psi^+(\{\bar{k}\},\{\bar{q}\}) + \psi^-(\{\bar{k}\},\{\bar{q}\})] - 4\pi|\bar{C}_{\bar{q}}|^2(\bar{\Omega} - \bar{q}_x\bar{u}_0)$$
$$\times \int_0^{+\infty} d\bar{k}_\perp \bar{k}_\perp \int_{-\infty}^{+\infty} d\bar{k}_x (\bar{k}_\perp^2 + \bar{k}_x^2)^{-1/2} \psi^-(\{\bar{k}\},\{\bar{q}\})$$
$$\times \left[\frac{\partial}{\partial \bar{\varepsilon}_{k_\perp}} + \frac{\partial}{\partial \bar{\varepsilon}_{k_x}}\right] \bar{f}(\bar{\varepsilon}_{k_\perp}, \bar{\varepsilon}_{k_x}). \tag{A12}$$

[1] H. Fröhlich and B. V. Paranjape, Proc. R. Soc. London, Ser. B **69**, 21 (1956).
[2] M. R. Arai, Appl. Phys. Lett. **42**, 906 (1983).
[3] X. L. Lei and C. S. Ting, Phys. Rev. B **32**, 1112 (1985).
[4] D. H. Huang, T. Apostolova, P. M. Alsing, and D. A. Cardimona, Phys. Rev. B **69**, 075214 (2004).
[5] C. S. Ting, S. C. Ying, and J. J. Quinn, Phys. Rev. B **14**, 4439 (1976).
[6] M. Artaki and P. J. Price, J. Appl. Phys. **65**, 1317 (1989).
[7] M. Lindberg and S. W. Koch, Phys. Rev. B **38**, 3342 (1988); J. V. Moloney, R. A. Indik, J. Hader, and S. W. Koch, J. Opt. Soc. Am. B **11**, 2023 (1999).
[8] X. L. Lei, H. L. Cui, and N. J. M. Horing, J. Phys. C **20**, L287 (1987).
[9] S. K. Lyo and D. H. Huang, Phys. Rev. B **66**, 155307 (2002).
[10] X. L. Lei and N. J. M. Horing, Phys. Rev. B **35**, 6281 (1987).
[11] J. Hader, J. V. Moloney, S. W. Koch, and W. W. Chow, IEEE J. Quantum Electron. **9**, 688 (2003).
[12] K. K. Thornber, J. Appl. Phys. **51**, 2127 (1980).
[13] X. L. Lei, J. Appl. Phys. **82**, 718 (1997); X. L. Lei, J. Appl. Phys. **84**, 1396 (1998).
[14] F. Q. Yan and X. L. Lei, J. Phys.: Condens. Matter **13**, 6625 (2001).
[15] X. L. Lei and S. Y. Liu, Phys. Rev. Lett. **91**, 226805 (2003).